

4

Internal Combustion Engines

Internal combustion engines are devices that generate work using the products of combustion as the working fluid rather than as a heat transfer medium. To produce work, the combustion is carried out in a manner that produces high-pressure combustion products that can be expanded through a turbine or piston. The engineering of these high-pressure systems introduces a number of features that profoundly influence the formation of pollutants.

There are three major types of internal combustion engines in use today: (1) the spark ignition engine, which is used primarily in automobiles; (2) the diesel engine, which is used in large vehicles and industrial systems where the improvements in cycle efficiency make it advantageous over the more compact and lighter-weight spark ignition engine; and (3) the gas turbine, which is used in aircraft due to its high power/weight ratio and also is used for stationary power generation.

Each of these engines is an important source of atmospheric pollutants. Automobiles are major sources of carbon monoxide, unburned hydrocarbons, and nitrogen oxides. Probably more than any other combustion system, the design of automobile engines has been guided by the requirements to reduce emissions of these pollutants. While substantial progress has been made in emission reduction, automobiles remain important sources of air pollutants. Diesel engines are notorious for the black smoke they emit. Gas turbines emit soot as well. These systems also release unburned hydrocarbons, carbon monoxide, and nitrogen oxides in large quantities.

In this chapter we examine the air pollutant emissions from engines. To understand the emissions and the special problems in emission control, it is first necessary that we understand the operating principles of each engine type. We begin our discussion with

a system that has been the subject of intense study and controversy—the spark ignition engine.

4.1 SPARK IGNITION ENGINES

The operating cycle of a conventional spark ignition engine is illustrated in Figure 4.1. The basic principle of operation is that a piston moves up and down in a cylinder, transmitting its motion through a connecting rod to the crankshaft which drives the vehicle. The most common engine cycle involves four strokes:

1. *Intake.* The descending piston draws a mixture of fuel and air through the open intake valve.

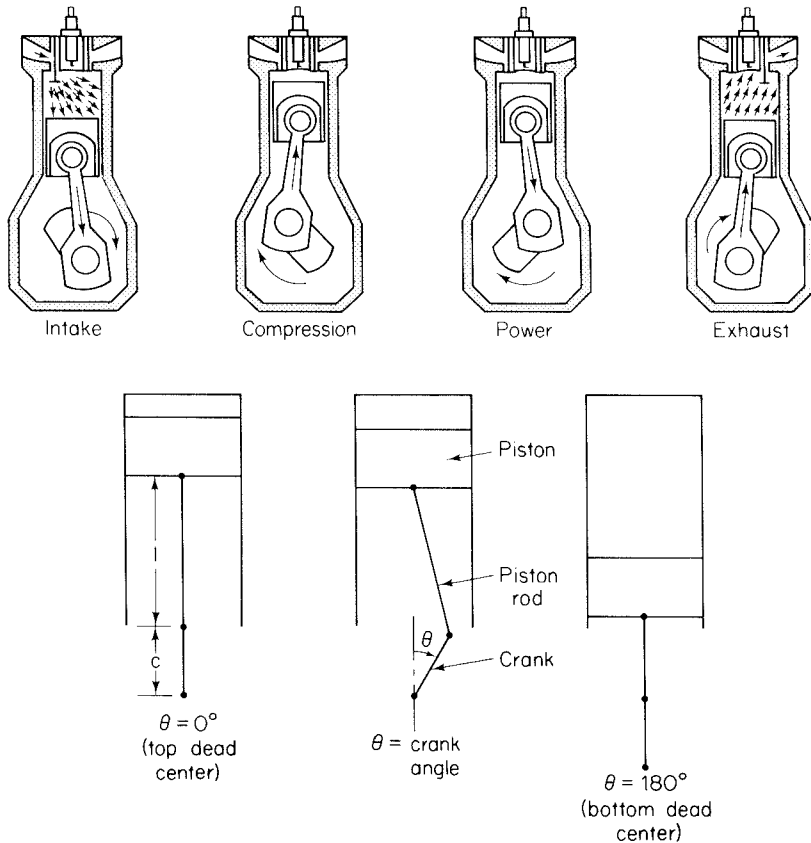


Figure 4.1 Four-stroke spark ignition engine: stroke 1, intake; stroke 2, compression; stroke 3, power; stroke 4, exhaust.

2. *Compression.* The intake valve is closed and the rising piston compresses the fuel-air mixture. Near the top of the stroke, the spark plug is fired, igniting the mixture.
3. *Expansion.* The burning mixture expands, driving the piston down and delivering power.
4. *Exhaust.* The exhaust valve opens and the piston rises, expelling the burned gas from the cylinder.

The fuel and air mixture is commonly premixed in a carburetor. Figure 4.2 shows how engine power and fuel consumption depend on equivalence ratio over the range commonly used in internal combustion engines. Ratios below 0.7 and above 1.4 generally are not combustible on the time scales available in reciprocating engines. The maximum power is obtained at a higher ratio than is minimum fuel consumption. As a vehicle accelerates, high power is needed and a richer mixture is required than when cruising at constant speed. We shall return to the question of the equivalence ratio when we consider pollutant formation, since this ratio is one of the key factors governing the type and quantity of pollutants formed in the cylinder.

The ignition system is designed to ignite the air-fuel mixture at the optimum instant. Prior to the implementation of emission controls, engine power was the primary concern in ignition timing. As engine speed increases, optimal power output is achieved

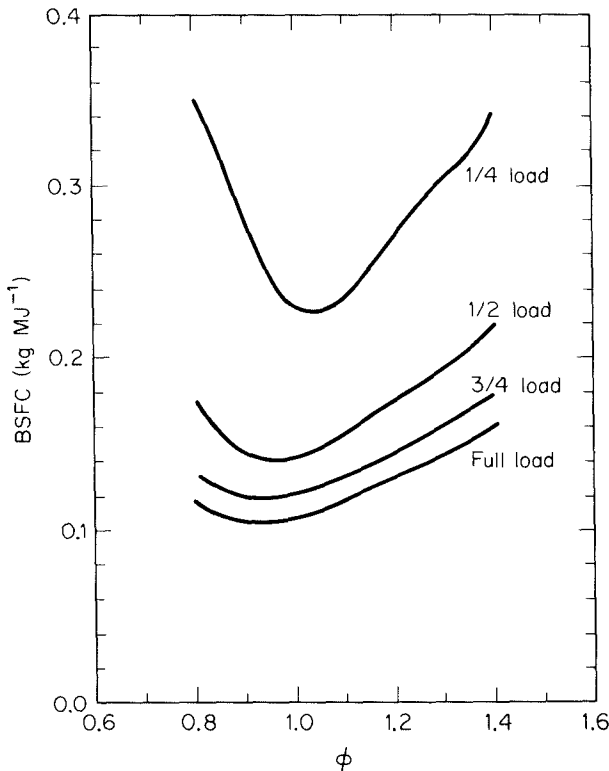


Figure 4.2 Variation of actual and indicated specific fuel consumption with equivalence ratio and load. BSFC denotes “brake specific fuel consumption.”

by advancing the time of ignition to a point on the compression stroke before the piston reaches the top of its motion where the cylinder volume is smallest. This is because the combustion of the mixture takes a certain amount of time, and optimum power is developed if the completion of the combustion coincides with the piston arriving at so-called top dead center. The spark is automatically advanced as engine speed increases. Also, a pressure diaphragm senses airflow through the carburetor and advances the spark as airflow increases.

Factors other than power output must be taken into account, however, in optimizing the engine operation. If the fuel–air mixture is compressed to an excessive pressure, the mixture temperature can become high enough that the preflame reactions can ignite the charge ahead of the propagating flame front. This is followed by very rapid combustion of the remaining charge and a correspondingly fast pressure increase in the cylinder. The resultant pressure wave reverberates in the cylinder, producing the noise referred to as *knock* (By et al., 1981). One characteristic of the fuel composition is its tendency to autoignite, expressed in terms of an octane rating.

High compression ratios and ignition spark timing that optimize engine power and efficiency lead to high octane requirements. The octane requirement can be reduced by using lower compression ratios and by delaying the spark until after the point for optimum engine performance. Emission controls require additional compromises in engine design and operation, sacrificing some of the potential engine performance to reduce emissions.

4.1.1 Engine Cycle Operation

The piston sweeps through a volume that is called the displacement volume, V_d . The minimum volume occurs when the piston is in its uppermost position. This volume is called the clearance volume, V_c . The maximum volume is the sum of these two. The ratio of the maximum volume to the clearance volume is called the compression ratio,

$$R_c = \frac{V_c + V_d}{V_c} \quad (4.1)$$

The efficiency of the engine is a strong function of the compression ratio. We shall see that R_c also has a strong influence on the formation of pollutants. The volume in the cylinder can be expressed as a simple function of the crank angle, θ , and the ratio of the length of the piston rod to that of the crank, that is,

$$V = V_c + \frac{V_d}{2} \left(1 + \frac{l}{c} - \cos \theta - \sqrt{\frac{l^2}{c^2} - \sin^2 \theta} \right) \quad (4.2)$$

where l is the piston rod length and c is the length of the crank arm as defined in Figure 4.1. The minimum volume occurs at $\theta = 0^\circ$, commonly referred to as *top dead center*, TDC. The maximum volume occurs at *bottom dead center*, BDC, $\theta = 180^\circ$. These positions are illustrated in Figure 4.1.

Engine speeds range from several hundred revolutions per minute (rpm) for large

industrial engines to 10,000 rpm or more for high-performance engines. Most automobiles operate with engine speeds in the vicinity of 3000 rpm. At this speed, each stroke in the cycle takes place in 20 ms. As an automobile is driven, the equivalence ratio and intake pressure vary with the engine load. Such changes in engine operation, however, are slow by comparison with the individual strokes. In discussing engine operation, we can assume that in any one cycle the engine operates at constant speed, load, and equivalence ratio.

We begin with a discussion of the thermodynamics of the spark ignition engine cycle and develop a model that has been used extensively in optimizing engine operation to minimize emissions and to maximize performance.

The spark ignition engine is one of the few combustion systems that burns premixed fuel and air. Fuel is atomized into the air as it flows through a carburetor and vaporizes before it enters the cylinder. Even though the fuel and air are premixed prior to combustion, the gas in the cylinder becomes segmented into burned and unburned portions once ignition occurs. A flame front propagates through the cylinder as illustrated in Figure 4.3. The fuel-air mixture ahead of the flame is heated somewhat by adiabatic compression as the burning gas expands. Not only are the burned and unburned gases at widely different temperatures, but also there are large variations in the properties of the burned gases. These variations must be taken into account to predict accurately the formation and destruction of NO_x and CO in the engine.

Another important feature that distinguishes reciprocating engines from the systems discussed thus far is that the volume in which the combustion proceeds is tightly constrained. While the individual elements of fluid do expand as they burn, this expansion requires that other elements of fluid, both burned and unburned, be compressed. As a result, the burning element of fluid does work on the other fluid in the cylinder, $\delta W = p dV$, increasing its internal energy and therefore its temperature.

While the engine strokes are brief, the time is still long by comparison with that required for pressure equilibration. For an ideal gas, the propagation rate for small pressure disturbances is the speed of sound,

$$a_s = \sqrt{\gamma RT/M} \quad (4.3)$$

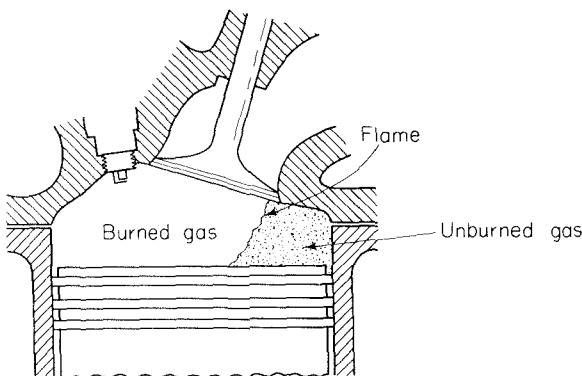


Figure 4.3 Flame propagation in the cylinder.

where γ is the ratio of specific heats, c_p/c_v , and M is the molecular weight of the gas; a_s is of the order of 500 to 1000 m s⁻¹ for typical temperatures in internal combustion engines. For a cylinder 10 cm in diameter, the time required for a pressure disturbance to propagate across the cylinder is on the order of 0.2 ms, considerably shorter than the time required for the stroke. Thus, to a first approximation, we may assume that the pressure is uniform throughout the cylinder at any instant of time, at least during normal operation.

4.1.2 Cycle Analysis

The essential features of internal combustion engine operation can be seen with a ‘‘zero-dimensional’’ thermodynamic model (Lavoie et al., 1970; Blumberg and Kummer, 1971). This model describes the thermodynamic states of the burned and unburned gases as a function of time, but does not attempt to describe the complex flow field within the cylinder.

We consider a control volume enclosing all the gases in the cylinder. Mass may enter the control volume through the intake valve at flow rate, \bar{f}_i . Similarly, mass may leave through the exhaust valve and possibly through leaks at a flow rate \bar{f}_e . The first law of thermodynamics (2.8) for this control volume may be written in the general form

$$\frac{dU}{dt} = \bar{f}_i \bar{h}_i - \bar{f}_e \bar{h}_e + \frac{dQ}{dt} - \frac{dW}{dt}$$

where U is the total internal energy of the gases contained in the cylinder and \bar{h}_i and \bar{h}_e are the mass specific enthalpies of the incoming and exiting flows, respectively. Q denotes the heat transferred to the gases. The work done by the gases, W , is that of a pressure acting through a change in the volume of the control volume as the piston moves. If we limit our attention to the time between closing the intake valve and opening the exhaust valve and assume that no leaks occur, no mass enters or leaves the cylinder (i.e., $\bar{f}_i = \bar{f}_e = 0$). The energy equation then simplifies to

$$\frac{d}{dt} (m \bar{u}_T) = \frac{dQ}{dt} - p \frac{dV}{dt}$$

where \bar{u}_T is the total mass specific internal energy (including energies of formation of all species in the cylinder), $-Q$ is heat transferred out of the charge, and m is the total mass of the charge. The only work done by the gases is due to expansion against the piston, so the work is expressed as $p dV/dt$. If we further limit our attention to constant engine speed, the time derivations may be expressed as

$$\frac{d}{dt} = \omega \frac{d}{d\theta}$$

where ω is the engine rotation speed (crank angle degrees per s). Thus we have

$$\frac{d}{d\theta} (m \bar{u}_T) = \frac{dQ}{d\theta} - p \frac{dV}{d\theta} \quad (4.4)$$

The total specific internal energy of the gas includes contributions of burned and unburned gases, with a mass fraction α of burned gas,

$$\bar{u}_T = \alpha \langle \bar{u}_b \rangle + (1 - \alpha) \langle \bar{u}_u \rangle \quad (4.5)$$

where $\langle \rangle$ denotes an average over the entire mass of burned or unburned gas in the cylinder. The unburned gas is quite uniform in temperature (i.e., $\langle \bar{u}_u \rangle = \bar{u}_u$) but the burned gas is not. Due to the progressive burning, a temperature gradient develops in the burned gas. As a fluid element burns, its expansion compresses both unburned and burned gases. Because the volume per unit mass of the hot burned gas is larger than that of the cooler unburned gas, the increase in the mass specific internal energy due to the compression work is higher for burned gas than for unburned gas. Therefore, we need to keep track of when individual fluid elements burn. Let $\bar{u}_b(\alpha, \alpha')$ represent the energy when the combustion has progressed to burned gas mass fraction α of a fluid element that burned when the burned gas mass fraction was α' . Averaging over all burned gas, we find

$$\langle \bar{u}_b \rangle(\alpha) = \int_0^\alpha \bar{u}_b(\alpha, \alpha') d\alpha' \quad (4.6)$$

The internal energy of either burned or unburned gas may be expressed in terms of the specific heat,

$$\bar{u}_i = \Delta \bar{u}_{f_i}^\circ(T_0) + \int_{T_0}^T \bar{c}_{v_i}(T') dT' \quad (4.7)$$

While the specific heats vary with temperature, we have already seen in Chapter 2 that variation is small over a limited temperature range. We assume constant specific heats since that will greatly simplify our analysis of the engine cycle. To minimize the errors introduced by this simplification, the specific heats should be evaluated for the actual composition of the gases in the cylinder as an average over the temperature range encountered by those gases. In terms of the linear correlations of specific heats presented in Table 2.5 and evaluating over the temperature interval, $T_1 \leq T \leq T_2$, this average becomes

$$\bar{c}_{v_i} = \frac{\int_{T_1}^{T_2} (a_i + b_i T) dT}{M_i (T_2 - T_1)} = \frac{a_i}{M_i} + \frac{b_i}{2M_i} (T_1 + T_2) \quad (4.8)$$

The internal energies of the burned and unburned portions of the gas may be expressed in terms of the average specific heats by

$$\begin{aligned} \bar{u}_b &= a_b + \bar{c}_{v_b} T_b \\ \bar{u}_u &= a_u + \bar{c}_{v_u} T_u \end{aligned} \quad (4.9)$$

where a_u and a_b include the reference temperature terms and the energies of formation. Substituting into (4.6), the mean burned gas energy becomes

$$\langle \bar{u}_b \rangle = \int_0^\alpha [a_b + \bar{c}_{vb} T_b(\alpha, \alpha')] d\alpha'$$

where $T_b(\alpha, \alpha')$ is the temperature of an element that burned at α' at a later time when combustion has progressed to α . Thus the mean burned gas energy can be expressed in terms of the mean burned gas temperature,

$$\langle \bar{u}_b \rangle = a_b + \bar{c}_{vb} \langle T_b \rangle \quad (4.10)$$

where

$$\langle T_b \rangle = \int_0^\alpha T_b(\alpha, \alpha') d\alpha'$$

Substitution of (4.5), (4.9), and (4.10) into the energy equation yields

$$\frac{d}{d\theta} [m(1 - \alpha)(a_u + \bar{c}_{vu} T_u) + m\alpha(a_b + \bar{c}_{vb} \langle T_b \rangle)] = \frac{dQ}{d\theta} - p \frac{dV}{d\theta} \quad (4.11)$$

The total volume of burned and unburned gases must, at all times, equal the volume in the cylinder:

$$V = m\alpha \langle \bar{v}_b \rangle + m(1 - \alpha) \bar{v}_u \quad (4.12)$$

Assuming ideal gases with constant composition, the mean specific volume of the burned gas is

$$\langle \bar{v}_b \rangle = \int_0^\alpha \frac{\bar{R}_b T_b(\alpha, \alpha')}{p} d\alpha' = \frac{\bar{R}_b \langle T_b \rangle}{p} \quad (4.13)$$

Noting that $\bar{R}_b = (\gamma_b - 1) \bar{c}_{vb}$, where $\gamma_b = \bar{c}_{pb} / \bar{c}_{vb}$ is the ratio of specific heats, (4.12) may now be simplified to

$$m\alpha \bar{c}_{vb} \langle T_b \rangle = \frac{pV}{\gamma_b - 1} - m(1 - \alpha) \frac{\gamma_b - 1}{\gamma_u - 1} \bar{c}_{vu} T_u \quad (4.14)$$

Substituting this result into (4.11) eliminates the burned gas temperature from the energy equation:

$$\begin{aligned} \frac{d}{d\theta} \left[m(1 - \alpha) a_u + m(1 - \alpha) \left(\frac{\gamma_b - \gamma_u}{\gamma_b - 1} \right) \bar{c}_{vu} T_u \right. \\ \left. + m\alpha a_b + \frac{pV}{\gamma_b - 1} \right] = \frac{dQ}{d\theta} - p \frac{dV}{d\theta} \end{aligned} \quad (4.15)$$

A simple approach can be used to eliminate the unburned gas temperature. At the end of the intake stroke, the cylinder is assumed to be filled with a uniform mixture of fuel and air and possibly some combustion products from previous cycles. The pressure, cylinder volume, and gas temperature at the time the intake valve closes are p_i , V_i , and T_i , respectively. Because the temperature difference between these gases and the cylinder wall is small (at least compared to that between combustion products and the wall),

compression of these gases is approximately adiabatic. Prior to firing the spark at θ_0 , the pressure in the cylinder can be determined from the formula for the relation between pressure and volumes in adiabatic compression,

$$p(\theta) = p_i \left[\frac{V_i}{V(\theta)} \right]^{\gamma_u} \quad \theta_i \leq \theta \leq \theta_0 \quad (4.16)$$

The temperature of the unburned gas throughout the cycle is that determined by adiabatic compression

$$T_u(\theta) = T_i \left[\frac{p(\theta)}{p_i} \right]^{-(\gamma_u - 1)/\gamma_u} \quad (4.17)$$

Substituting (4.17) into (4.15) and differentiating yield

$$\begin{aligned} & m(1 - \alpha) \frac{\gamma_b - \gamma_u}{\gamma_b - 1} \bar{c}_{vu} T_i \left(\frac{p}{p_i} \right)^{(\gamma_u - 1)/\gamma_u} \frac{1}{p} \frac{\gamma_u - 1}{\gamma_u} \frac{dp}{d\theta} \\ & + m \left[a_b - a_u - \frac{\gamma_b - \gamma_u}{\gamma_b - 1} \bar{c}_{vu} T_i \left(\frac{p}{p_i} \right)^{(\gamma_u - 1)/\gamma_u} \right] \frac{d\alpha}{d\theta} \\ & + \frac{p}{\gamma_b - 1} \frac{dV}{d\theta} + \frac{V}{\gamma_b - 1} \frac{dp}{d\theta} \\ & = \frac{dQ}{d\theta} - p \frac{dV}{d\theta} \end{aligned} \quad (4.18)$$

This equation may be rearranged to express the rate of change of the cylinder pressure in terms of the conditions at the end of the intake stroke, the rate of volume change, and the combustion and heat transfer rates, that is,

$$\frac{dp}{d\theta} = \frac{\frac{dQ}{d\theta} - \frac{\gamma_b}{\gamma_b - 1} p \frac{dV}{d\theta} - m \left[a_b - a_u - \frac{\gamma_b - \gamma_u}{\gamma_b - 1} \bar{c}_{vu} T_i \left(\frac{p}{p_i} \right)^{(\gamma_u - 1)/\gamma_u} \right] \frac{d\alpha}{d\theta}}{m(1 - \alpha) \bar{c}_{vu} \frac{\gamma_b - \gamma_u}{\gamma_b - 1} \frac{\gamma_u - 1}{\gamma_u} \frac{T_i}{p} \left(\frac{p}{p_i} \right)^{(\gamma_u - 1)/\gamma_u} + \frac{V}{\gamma_b - 1}} \quad (4.19)$$

4.1.3 Cylinder Turbulence and Combustion Rate

We need to know the combustion rate, $d\alpha/d\theta$, to use the model of (4.19). To efficiently convert the heat released by combustion to work on the piston, the charge must be burned completely in the early part of the expansion stroke. The duration of the stroke in automotive engines is on the order of 20 ms, so the combustion can take at most a few milliseconds. Since typical laminar flame speeds are less than 1 m s^{-1} , tens of milliseconds would be required for laminar flame propagation across a cylinder several centimeters in diameter. We see, therefore, that the acceleration of flame propagation that turbulence provides is essential to efficient engine operation.

As discussed in Chapter 2, the turbulent flame speed depends on the turbulent intensity, u' . The turbulent intensity is governed by engine design and operation, and varies during the stroke as described below. The mixture entrained in the flame front by the turbulent motion burns at a rate that depends on combustion kinetics through the laminar flame speed, S_L . The laminar flame speed peaks near stoichiometric and decreases for richer or leaner mixtures, so there is also some dependence of flame speed on the equivalence ratio. To make general statements about the factors governing pollutant formation in spark ignition engines, therefore, we need to understand how turbulence varies with engine operation.

The generation of turbulence in an internal combustion engine is a complex, unsteady process. As the mixture passes through the intake valve, the flow separates, resulting in a highly unsteady motion (Hoult and Wong, 1980). The intensity of the resulting turbulent motion depends on the detailed geometry of the intake port and valve, on the geometry of the cylinder and piston, and on the speed of the piston.

As we discussed in Chapter 2, the turbulence may be characterized in terms of two quantities: (1) the turbulent kinetic energy per unit mass

$$E_k = \frac{1}{2} (\overline{u_1^2} + \overline{u_2^2} + \overline{u_3^2}) \quad (4.20)$$

which describes the large-scale behavior of the turbulence, and (2) the rate of turbulent kinetic energy dissipation

$$\epsilon = \nu \left[\overline{\frac{\partial u'_i}{\partial x_j} \frac{\partial u'_i}{\partial x_j}} \right] \quad (4.21)$$

which describes the effects of the small-scale turbulent motions.

The mixture passes through the intake valve at a velocity that is proportional to the piston speed and hence to the angular rotation speed, ω . The kinetic energy of this incoming flow contributes to the turbulent kinetic energy within the cylinder. How much of that kinetic energy remains at bottom dead center when the compression begins depends on the geometry of the particular engine.

The turbulent kinetic energy is not constant during the compression and power strokes. Dissipation tends to decrease E_k , while the distortion due to compression of the existing turbulent field tends to increase it. Turbulent kinetic energy may also be produced by shear associated with fluid motions. Shrouds on the intake valves, illustrated in Figure 4.4, are used to create a swirling motion in the cylinder. Complex piston or cylinder head shapes induce fluid motions during the final approach to top dead center, also shown in Figure 4.4. This so-called *squish* can greatly enhance the turbulent kinetic energy level immediately prior to combustion.

Neglecting diffusion of the turbulent kinetic energy, the rate of change of the turbulent kinetic energy is a balance between production and dissipation:

$$\rho \frac{dE_k}{dt} = \rho P - \rho \epsilon \quad (4.22)$$

where P is the rate of turbulent kinetic energy production.

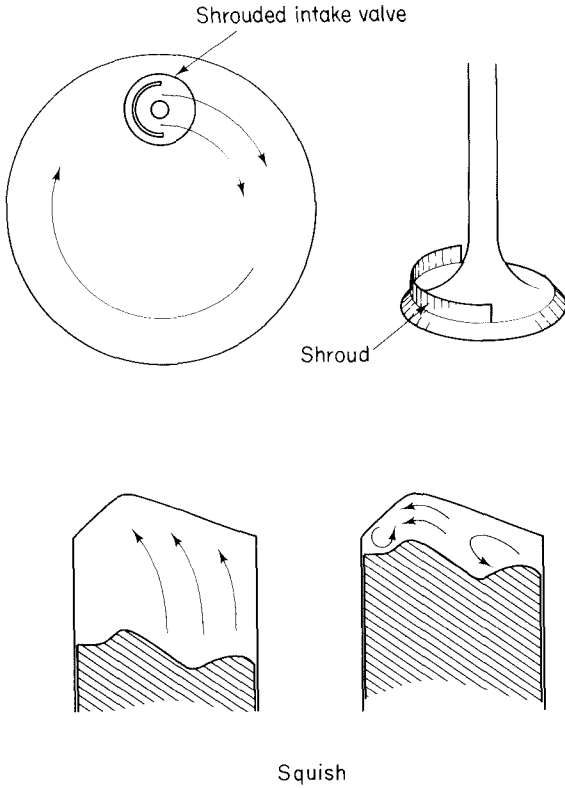


Figure 4.4 Valve, head, and piston design features that enhance mixing.

The dissipation rate was shown in Appendix D of Chapter 1 to be related to u' for homogeneous, isotropic turbulence,

$$\epsilon \approx \nu \frac{u'^2}{\lambda^2} \approx \frac{u'^3}{l}$$

where λ and l are the Taylor microscale and integral scale, respectively. Using the definition of E_k , we find

$$\epsilon \approx \frac{E_k^{3/2}}{l} \tag{4.23}$$

Assuming that angular momentum in the turbulent field is conserved during the rapid compression:

$$u'l \approx E_k^{1/2}l \approx \text{const.}$$

we see that ϵ is proportional to E_k^2 ,

$$\epsilon \propto E_k^2 \tag{4.24}$$

The gas density and integral scale are related by conservation of mass,

$$\rho l^3 = \text{const.}$$

or

$$l \propto \rho^{-1/3} \quad (4.25)$$

Using (4.24), this yields

$$u' \propto \rho^{1/3} \quad (4.26)$$

or

$$E_k \propto \rho^{2/3} \quad (4.27)$$

We may use these scaling arguments to simplify the rate equation for the turbulent kinetic energy. Assuming that due to the rapid distortion of the flow caused by the compression due to both piston motion and the expansion of gases upon burning, the production of turbulent kinetic energy is much more rapid than its dissipation (Borgnakke et al., 1980),

$$\rho P \approx \rho \frac{dE_k}{dt}$$

and applying (4.27), the production of turbulent kinetic energy due to the rapid distortion of the turbulent field during compression, yields

$$P \approx \frac{2}{3} \frac{E_k}{\rho} \frac{d\rho}{dt} \quad (4.28)$$

The rate equation for E_k becomes

$$\frac{dE_k}{dt} = \frac{2}{3} \frac{E_k}{\rho} \frac{d\rho}{dt} - CE_k^2 \quad (4.29)$$

where ϵ has been eliminated using (4.24).

The production term generally dominates during the compression and combustion processes due to the rapid change in density, so (4.29) may be rewritten as

$$\omega \frac{d \ln (E_k/E_{k0})}{d\theta} \approx \omega \frac{2}{3} \frac{d \ln (\rho/\rho_0)}{d\theta} \quad (4.30)$$

where E_{k0} and ρ_0 denote the initial kinetic energy and density. We see that the relative change of the turbulent kinetic energy from bottom dead center to any crank angle, θ , is, to a first approximation, independent of the crank rotation speed, ω . The initial turbulent kinetic energy depends on piston speed as

$$E_{k0} \approx \omega^2 \quad (4.31)$$

because the inlet flow velocity is proportional to the piston speed. Thus, for a given engine geometry, the value of u' at any crank angle, θ , is approximately proportional to the angular speed

$$u'_0 \approx \omega \quad (4.32)$$

and the turbulent flame propagation velocity increases with the engine speed.

This dependence of flame speed on engine speed means that the number of crank angle degrees required for combustion in a given engine does not depend strongly on the engine speed. Thus, if $\alpha(\theta)$ is known for one engine speed, we may use that result as an estimate of the burn rate for other engine speeds with reasonable confidence.

Rather than attempt to develop detailed fluid mechanical models of the combustion process, therefore, we shall simply specify a functional form for $\alpha(\theta)$ that exhibits the essential features of actual combustion profiles, that is, a delay from the time the spark is fired until the pressure rise associated with combustion becomes appreciable, an accelerating combustion rate until a large fraction of the charge is burned, followed by a decreasing burn rate. A simple function with this sigmoidal behavior is the cosine function,

$$\alpha(\theta) = \frac{1}{2} \left[1 - \cos \left(\frac{\theta - \theta_0}{\Delta\theta_c} \pi \right) \right] \quad \theta_0 \leq \theta \leq \theta_0 + \Delta\theta_c \quad (4.33)$$

where θ_0 is the crank angle at which the spark is fired and $\Delta\theta_c$ is the burn duration. Other functions that allow the shape of the combustion profile to be varied have been used in the literature, but this simple function is adequate for our present purpose of exploring engine operation. We do not attempt to predict the burn duration, since it is a complex function of engine design and operation.

4.1.4 Cylinder Pressure and Temperature

The pressure in the cylinder can be determined by integrating (4.19) with $\alpha(\theta)$ given by (4.33) or another suitable model and with an expression for the heat transfer $dQ/d\theta$. The heat transfer is also a function of the turbulent field (Borgnakke et al., 1980). For our present purposes, it is sufficient to assume that the engine is adiabatic (i.e., $dQ/d\theta = 0$).

Once the pressure in the cylinder is known the mean burned and unburned gas temperatures can be calculated using (4.14) and (4.17), respectively. The temperatures of individual burned gas elements can be calculated if it is assumed that no mixing of the burned gases occurs and that heat transfer from a burned gas element is negligible. Under these assumptions, the burned gases can be assumed to undergo adiabatic compression and expansion from the time they burn. The temperature of an element burned when the mass fraction burned was α' is

$$T_b(\alpha, \alpha') = T_b(\alpha', \alpha') \left[\frac{p(\alpha)}{p(\alpha')} \right]^{(\gamma_b - 1)/\gamma_b} \quad (4.34)$$

The temperature of the element immediately following combustion, $T_b(\alpha', \alpha')$, may be evaluated by applying the first law of thermodynamics to the combustion of an infinitesimal mass of charge, dm . For combustion of a sufficiently small incremental mass, the pressure change during combustion is insignificant. The enthalpy of the burned gas equals that for the unburned gas, that is,

$$\bar{h}_u = \bar{u}_u + \bar{R}_u T_u = \bar{h}_b = \bar{u}_b + \bar{R}_b T_b$$

The burned gas temperature becomes

$$T_b(\alpha', \alpha') = \frac{a_u - a_b + \bar{c}_{pu} T_u}{\bar{c}_{pb}} \tag{4.35}$$

From (4.19), (4.34), and (4.35) we can determine the pressure-temperature history of each element in the charge from the beginning to the end of combustion. Figure 4.5 shows the results of calculations of Heywood (1976) for an engine with a compression ratio of 7.0. The spark is fired at 40° before top dead center. The combustion duration, $\Delta\theta_c$, is 60°. The fraction of charge burned and the cylinder pressure are shown as a function of crank angle in Figure 4.5. The temperatures of the first and last gases to burn are shown as solid lines. The dashed curves represent the temperature of the unburned gas.

The first gas to burn rises to a high temperature immediately. As additional gas burns, the pressure in the cylinder rises, compressing both burned and unburned gases.

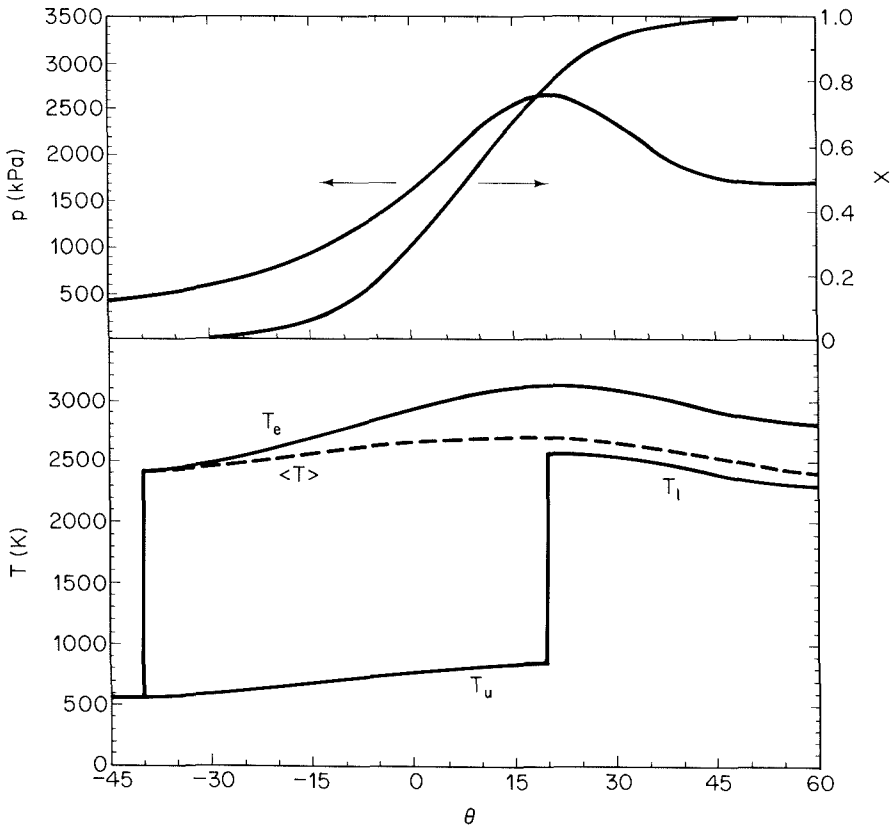


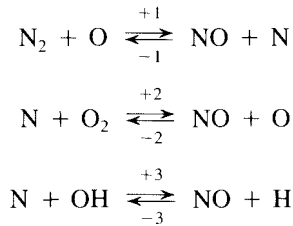
Figure 4.5 Burned mass fraction, cylinder pressure, and temperatures of the gas that burns early, T_e , late, T_l , and the mean gas temperature inside the cylinder (after Heywood, 1976).

The work done on a gas element by this compression is $p dV$. Because the volume of a mass of burned gas is larger than that of an equal mass of unburned gas, more work is done on the gas that burns early in the cycle than is done on that that burns at a later time. The first gas burned, therefore, is the hottest gas in the cylinder.

4.1.5 Formation of Nitrogen Oxides

The foregoing model simulates the essential features of the combustion in the spark ignition engine and provides a basis for understanding the formation of pollutants in the cylinder. We first examine the rate of NO formation. In Chapter 3 we saw that NO formation is highly temperature dependent, so we expect that the NO formation rate will vary with location in the charge, depending on the temperature history of each element. Since the NO reactions require the thermal energy released by the combustion process, NO formation will take place only in the burned gases.

The dominant reactions in NO formation are those of the extended Zeldovich mechanism:



Assuming that O, OH, and H are at their equilibrium concentration and that N atoms are at pseudo-steady state, we obtained the following rate equation for NO formation and decomposition (3.12):

$$\frac{dy_{\text{NO}}}{d\theta} = \frac{RT}{p} \omega \left[\frac{2R_1(1 - \beta^2)}{\beta R_1/(R_2 + R_3) + 1} \right] \quad (4.36)$$

where y_{NO} = mole fraction of NO

$\beta = y_{\text{NO}}/y_{\text{NO}_e}$, fractional attainment of equilibrium*

y_{NO_e} = equilibrium mole fraction of NO

R_i = forward reaction rate of reaction i evaluated at equilibrium conditions, $i = 1, 2, 3$

When $\beta < 1$ and $dy_{\text{NO}}/d\theta > 0$, NO tends to form; when $\beta > 1$ and $dy_{\text{NO}}/d\theta < 0$, NO tends to decompose. Equation (4.36) is integrated at each point α' in the charge from the crank angle at which that element initially burns to a crank angle at which the reaction rates are negligible. At this point the quenched value of the NO mole fraction

*We use β here as this fraction to avoid confusion with the fraction burned α .

y_{NO_q} is achieved. The overall mole fraction of NO in the entire charge is given by

$$\bar{y}_{NO} = \int_0^1 y_{NO_q}(\alpha') d\alpha' \tag{4.37}$$

Nitric oxide concentrations versus crank angle, computed by Blumberg and Kummer (1971), are shown in Figure 4.6. Both rate calculated and equilibrium NO are shown at three positions in the charge, $\alpha' = 0, 0.5, 1.0$. The major contribution to the total NO formed results from the elements that burn first. They experience the highest temperatures and have the longest time in which to react. Considerable decomposition of NO occurs in the first element because of the high temperatures. However, as the first element cools during expansion, the rate of NO decomposition rapidly decreases, so that after about 40 crank angle degrees, the NO kinetics are effectively frozen.

We can now summarize the processes responsible for the production of nitric oxide

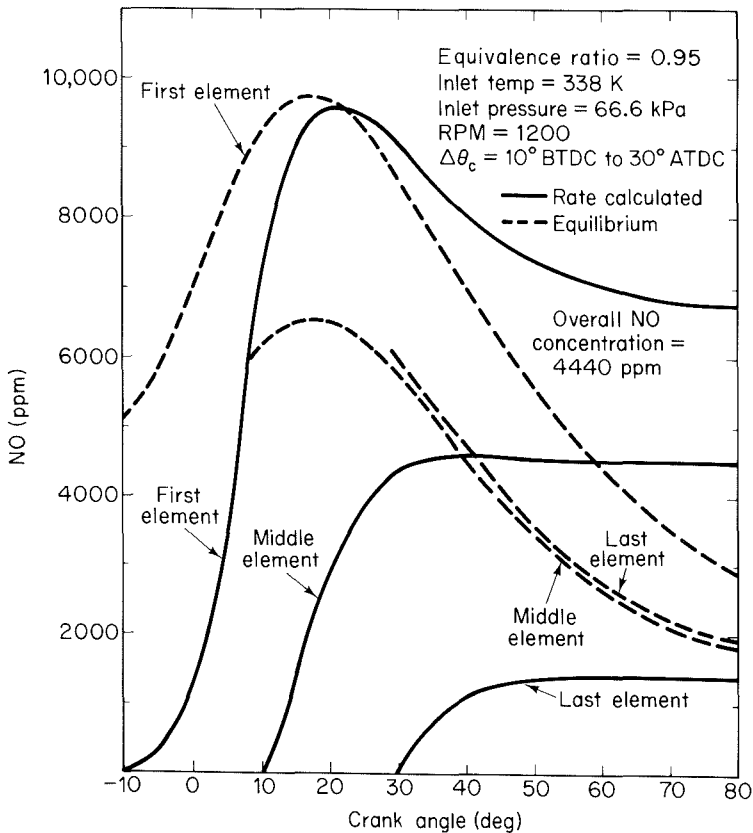


Figure 4.6 Nitric oxide concentration in the burned gas as a function of crank angle for the first, middle, and last element to burn for $\phi = 0.97$ (Blumberg and Kummer, 1971). Reprinted by permission of Gordon and Breach Science Publishers.

in the internal combustion engine. During the flame propagation, NO is formed by chemical reactions in the hot just-burned gases. As the piston recedes, the temperatures of the different burned elements drop sharply, “freezing” the NO (i.e., the chemical reactions that would remove the NO become much slower) at the levels formed during combustion, levels well above these corresponding to equilibrium at exhaust temperatures. As the valve opens on the exhaust stroke, the bulk gases containing the NO exit. It is to the processes that occur prior to the freezing of the NO levels that we must devote our attention if we wish to reduce NO formation in the cylinder.

4.1.6 Carbon Monoxide

The compression due to piston motion and combustion in a confined volume leads to very high burned gas temperatures in reciprocating engines. Peak temperatures may range from 2400 to 2800 K, with pressures of 15 to 40 atm. In Chapter 3 we saw that the C–H–O system equilibrates rapidly at such high temperatures. It is therefore reasonable to assume that CO is equilibrated immediately following combustion. The equilibrium CO mole fraction at these peak temperatures is very high, greater than 1%.

Work done by the gas in the cylinder on the piston during the expansion stroke cools the combustion products. When the exhaust valve first opens, the pressure in the cylinder is much larger than that in the exhaust manifold. As the gas is forced out through the valve, work is done by the gas remaining in the cylinder, so the temperature drops even more rapidly. Ultimately, this cooling of the combustion products exceeds the ability of the three-body and CO oxidation reactions to maintain equilibrium.

The combustion products are rapidly cooled during the expansion stroke and the exhaust process, causing the CO oxidation kinetics to be quenched while the CO level is still relatively high. In Chapter 3 it was shown that CO oxidation proceeds primarily by reaction with OH,



and that the OH can be present at concentrations significantly greater than that at equilibrium in rapidly cooled combustion products. The concentrations of OH and other radicals can be described using the partial-equilibrium model developed in Chapter 3, wherein it was shown that the rate of CO oxidation is directly coupled to the rates of the three-body recombination reactions, primarily,



in fuel-lean combustion. CO levels in spark ignition engines are generally high enough that the influence of the CO oxidation on the major species concentrations cannot be ignored. The direct minimization of the Gibbs free energy is better suited to incorporating this detail than is the equilibrium-constant approach developed in Chapter 3.

Heywood (1975) used the rate-constrained, partial-equilibrium model (based on direct minimization of the Gibbs free energy) to study CO behavior in spark ignition engines. His calculations confirm that at the peak temperatures and pressures the equilibration of CO is fast compared to the changes due to compression or expansion, so

equilibrium may reasonably be assumed immediately following combustion. The burned gases are not uniform in temperature, however; so the equilibrium CO level depends on when the element burned. Furthermore, the blowdown of the cylinder pressure to the exhaust manifold pressure in the initial phase of the exhaust process lasts about 90 crank angle degrees. Thus the temperature-time profiles of fluid elements within the charge differ depending on the time of burning and on when they pass from the cylinder through the valve into the exhaust manifold.

These effects are illustrated by the results of an idealized calculation shown in Figure 4.7. CO mole fractions for individual fluid elements in the burned gas mixture are shown as a function of crank angle. The elements are identified in terms of the fraction of the total charge burned when the element burned, α , and the mass fraction that has left the cylinder when the element leaves the cylinder, z . The partial-equilibrium calculations are close to equilibrium until about 50 crank angle degrees after top dead center, when the rapid cooling due to adiabatic expansion leads to partial quenching of the CO oxidation.

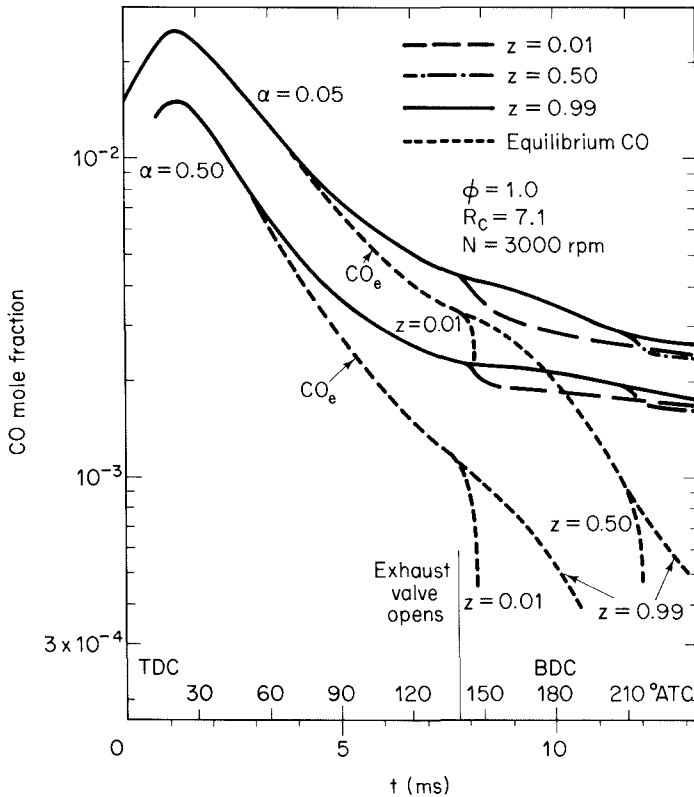


Figure 4.7 Carbon monoxide concentration in two elements in the charge that burn at different times, during expansion and exhaust processes. α is the mass fraction burned and z is the fraction of the gas that has left the cylinder during the exhaust process (Heywood, 1975). Reprinted by permission of The Combustion Institute.

The CO levels measured in fuel-lean combustion are substantially higher than those predicted with the partial-equilibrium model, but agreement is good near stoichiometric (Heywood, 1976). In fuel-rich combustion, the CO levels in the exhaust gases are close to the equilibrium concentrations, as predicted by the partial-equilibrium model. The reasons for the high levels in fuel-lean combustion are not fully understood, but may be coupled to the oxidation of unburned hydrocarbons in the exhaust manifold.

4.1.7 Unburned Hydrocarbons

The range of equivalence ratios over which spark ignition engines operate is narrow, typically $0.7 < \phi < 1.3$, the fuel and air are premixed, and the flame temperatures are high. These conditions, in steady-flow combustion systems, generally would lead to very low emissions of unburned hydrocarbons. Why, then, are relatively large quantities of hydrocarbon gases present in the combustion products of automobile engines? This question has been the subject of numerous investigations in which hypotheses have been developed and supported with theory and experiment, only to be later challenged with new interpretations that contradict earlier models.

In an early investigation of this problem, Daniel and Wentworth (1962) magnified photographs of the flame spread in the cylinder of a spark ignition engine. It was observed that the flame failed to propagate through the mixture located within 0.1 to 0.7 mm of the cylinder wall. They hypothesized that this *wall quenching* allowed hydrocarbons to escape combustion in spark ignition engines.

Figure 4.8 shows the nature of these wall quench regions. In addition to the quench layers at the cylinder walls, the small volume between the piston and cylinder wall above the top piston ring, called the crevice volume, contains unburned hydrocarbons. Experiments were performed in which the quench zone of an operating engine was sampled. It was found that the proportion of the quench zone exhausted is less than that of the total gas exhausted. This observation was attributed to trapping in the boundary layer.

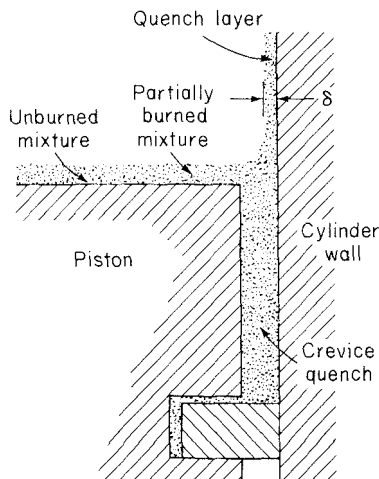


Figure 4.8 Schematic showing the quench layer and crevice volume where heat transfer to the walls may quench the combustion (Tabaczynski et al., 1972; © SAE, Inc.).

A fraction of the gas remains in the cylinder at the end of the exhaust stroke. Although this residual gas amounts to a small fraction of the total gas in the cylinder in a normally operating engine, the residual gas hydrocarbon concentration tends to be very high. The recycled hydrocarbons may be a significant fraction of the hydrocarbons left unburned in the cylinder.

The trapping effect can be explained as follows. Gases adjacent to the wall opposite the exhaust valve are the farthest from the exit and least likely to be exhausted. Gases along the walls near the exhaust valve have a better chance to be exhausted, but viscous drag slows their movement. Some quenched gases do escape, but on the whole the more completely burned gases at the center of the chamber are preferentially exhausted first, with the result that the residual gas has a higher concentration of hydrocarbons than the exhaust gas. It is likely that the quench zone hydrocarbons that remain in the cylinder are burned in the succeeding cycle. In the experiments reported by Daniel and Wentworth (1962), about one-third of the total hydrocarbons were recycled and probably burned in succeeding cycles.

Figure 4.9 shows the measured variation in the exhaust hydrocarbon concentration and mass flow rate with crank angle. As the exhaust valve opens and the emptying of the combustion chamber starts, the hydrocarbon concentration in the exhaust manifold increases rapidly to a peak of 600 ppm. The hydrocarbon concentration then drops and remains at 100 to 300 ppm for much of the exhaust stroke. Late in the exhaust stroke, the hydrocarbon level again rises sharply. The hydrocarbon mass flow rate shows two distinct peaks corresponding to these concentration maxima. The early peak in the hydrocarbon concentration was attributed to the entrainment of the quench layer gases near the exhaust valve immediately after it opens. The low hydrocarbon concentration during the middle portion of the exhaust stroke is most probably due to the release of burned gases from the center of the cylinder.

Tabaczynski et al. (1972) further observed that, during the expansion stroke, the gases in the crevice volumes are laid along the cylinder wall. As the piston moves up during the exhaust stroke, the layer is scraped off the wall and rolled up into a vortex, as depicted in Figure 4.10. The second peak in the hydrocarbon concentration was attributed to the passage of this vortex through the exhaust valve late in the exhaust stroke.

Although the quench layer model does appear to explain many of the observations of hydrocarbons in spark ignition engines, recent studies have questioned the importance of quench layers as sources of unburned hydrocarbons (Lavoie et al., 1980). The cooling effect of the wall does, indeed, prevent the flame from propagating all the way to the cylinder wall. Hydrocarbon vapors can diffuse from this cool region, however, into the hotter gases farther from the wall. If this occurs early in the cycle when the temperature of the burned gases is high, the hydrocarbons from the quench layer will be burned.

We can gain some insight into the quench-layer problem by examining the time scales of diffusion and reaction of the hydrocarbon gases. The characteristic time for diffusion of gases from the quench layer into the bulk gases is $\tau_D \approx \delta^2/D$. Adamczyk and Lavoie (1978) report values of δ of order 50 to 75 μm and diffusion times ranging from 0.1 to 0.3 ms at atmospheric pressure. Inasmuch as this time is short compared to that of the expansion stroke and typical combustion times, a considerable amount of the

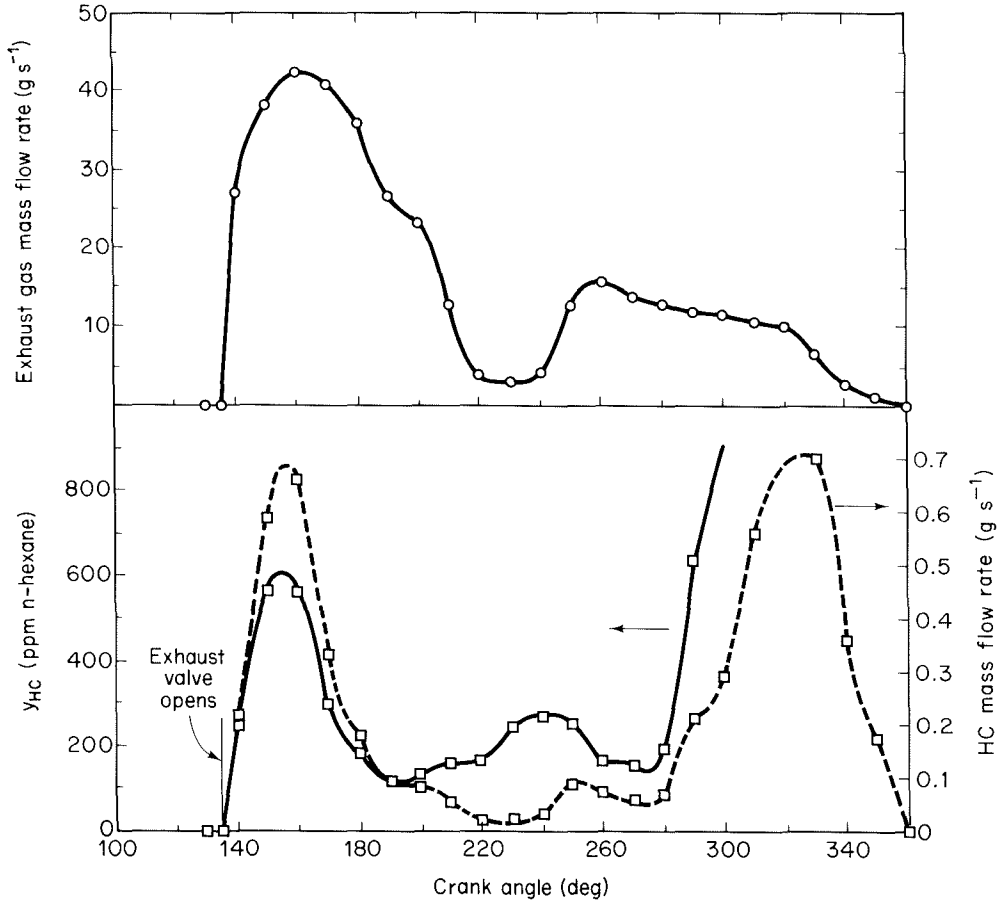


Figure 4.9 Measured instantaneous mass flow rate exhaust hydrocarbon concentration, and hydrocarbon mass flow rate out of the exhaust valve (Tabaczynski et al., 1972; © SAE, Inc.).

quench layer hydrocarbons may be expected to diffuse away from the walls and burn in the cylinder. Some quench-layer hydrocarbons may survive because the thermal boundary layer spreads at a rate comparable to that of the hydrocarbons, preventing the hydrocarbons from reaching high temperatures at which they would rapidly oxidize. The quantities of hydrocarbons that survive by this route, however, are much too small to explain the observed hydrocarbon levels. In one study in which the quench-layer gases were sampled directly, it was estimated that the quench-layer gases could account for not more than 3 to 12% of the hydrocarbons measured in the exhaust (LoRusso et al., 1983).

Hydrocarbons contained in the crevice volume between the piston, piston ring, and cylinder wall account for much of the hydrocarbon release. These vapors expand out from the crevices late in the expansion stroke, so lower temperatures are encountered

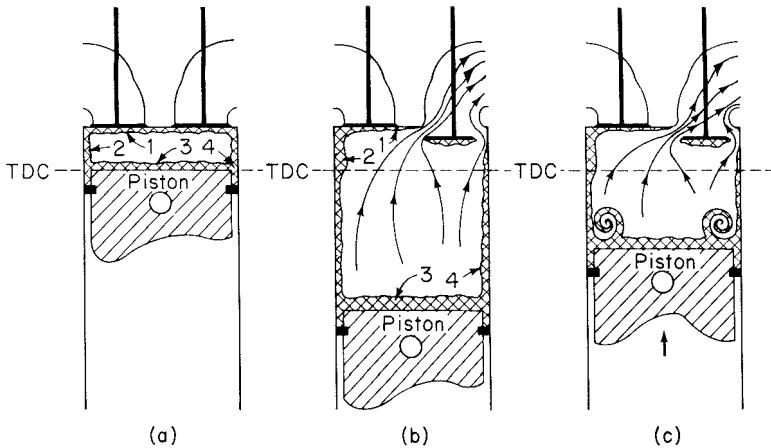


Figure 4.10 Schematic illustrating the quench layer model for hydrocarbon emissions. (a) Quench layers are formed as heat transfer extinguishes the flame at the cool walls and in the crevice volume. (b) Gas in the crevice volume expands and is spread along the cylinder wall as the pressure falls. When the exhaust valve opens, the quench layers near the valve exit the cylinder. (c) The hydrocarbon-rich cylinder wall boundary layer rolls up into a vortex as the piston moves up the cylinder during the exhaust stroke (Tabaczynski et al., 1972; © SAE, Inc.).

by crevice gases than by the quench-layer gases (Wentworth, 1971). Adamczyk et al. (1983) examined the retention of hydrocarbons in a combustion bomb that consisted of a fixed piston in an engine cylinder. About 80% of the hydrocarbons remaining after combustion were attributed to the piston crevice, with most of the remaining hydrocarbons surviving in smaller crevices associated with the head gasket and with the threads on the spark plug. The crevice volumes contribute primarily to the peak in the hydrocarbon flux late in the exhaust process, since those gases originate far from the exhaust valve.

Other sources must therefore contribute significantly to the hydrocarbon emissions, particularly those that exit the cylinder early in the exhaust process. Haskell and Legate (1972) and Wentworth (1968) suggested that lubricating oil layers on the cylinder walls may adsorb or dissolve hydrocarbon vapors during the compression stroke. These stored hydrocarbons are protected from the flame. As the pressure in the cylinder drops during the expansion stroke and exhaust process, these hydrocarbons desorb into the combustion products. Kaiser et al. (1982) showed that fuel vapors and fuel hydrocarbon oxidation product emissions increase as the amount of oil in the cylinder increases. Carrier et al. (1981) developed a model for cyclic hydrocarbon adsorption and desorption in a liquid film, taking into account thermodynamic equilibrium at the gas-liquid interface and diffusional resistance within the liquid layer. The results from this model are qualitatively consistent with the observed reduction of hydrocarbon emission with engine speed.

4.1.8 Combustion-Based Emission Controls

The equivalence ratio has a strong influence on the formation of nitrogen oxides and on the oxidation of carbon monoxide and unburned hydrocarbons, but the extent to which these emissions can be controlled through fuel–air ratio adjustment alone is limited. Other combustion parameters that can influence emissions include the ignition timing and design parameters. The compression ratio determines the peak pressure and hence the peak temperature in the cycle. The piston and cylinder head shapes and the valve geometry influence the turbulence level in the engine and therefore the rate of heat release during combustion. Temperatures can also be reduced through dilution of the incoming air with exhaust gases.

Design and operating variables not only influence the levels of pollutant emissions, but also directly affect the engine power output and efficiency. As we examine various emission control strategies, we must also examine their effects on engine performance. The efficiency of an internal combustion engine is generally reported in terms of the *specific fuel consumption* (SFC), the mass of fuel consumed per unit of energy output, kg MJ^{-1} or g kW-h^{-1} . The work output per engine cycle is presented in terms of the *mean effective pressure* (MEP), the work done per displacement volume. If the MEP is determined in terms of the net power output, P , the quantity is called the *brake mean effective pressure* (BMEP) and is calculated as

$$\text{BMEP} = \frac{2P}{V_d \Omega} \quad (4.38)$$

where Ω is the engine rotation speed (revolutions per second). Many factors not directly involved in the combustion process influence the BMEP: friction; pumping work associated with the intake and exhaust flows; and work used to drive engine equipment such as generators, water pumps, fans, and so on. The work performed by the gas during the compression and expansion strokes,

$$W_i = \int_{0^\circ}^{360^\circ} p \frac{dV}{d\theta} d\theta \quad (4.39)$$

that is, that that would be *indicated* by a pressure measurement, is of more concern to us here. The mean effective pressure based on this work,

$$\text{IMEP} = \frac{W_i}{V_d} \quad (4.40)$$

is called the *indicated mean effective pressure* (IMEP). It is also convenient to present the specific fuel consumption in terms of the indicated work to eliminate the influences of parasitic losses and loads. This quantity is then called the *indicated specific fuel consumption* (ISFC).

Figure 4.11 shows the influence of engine operating equivalence ratio on the indicated specific NO_x emissions ($\text{g NO}_x \text{ MJ}^{-1}$) and fuel consumption for three different values of the combustion duration. NO_x emissions are maximum at $\phi = 1$ and decrease

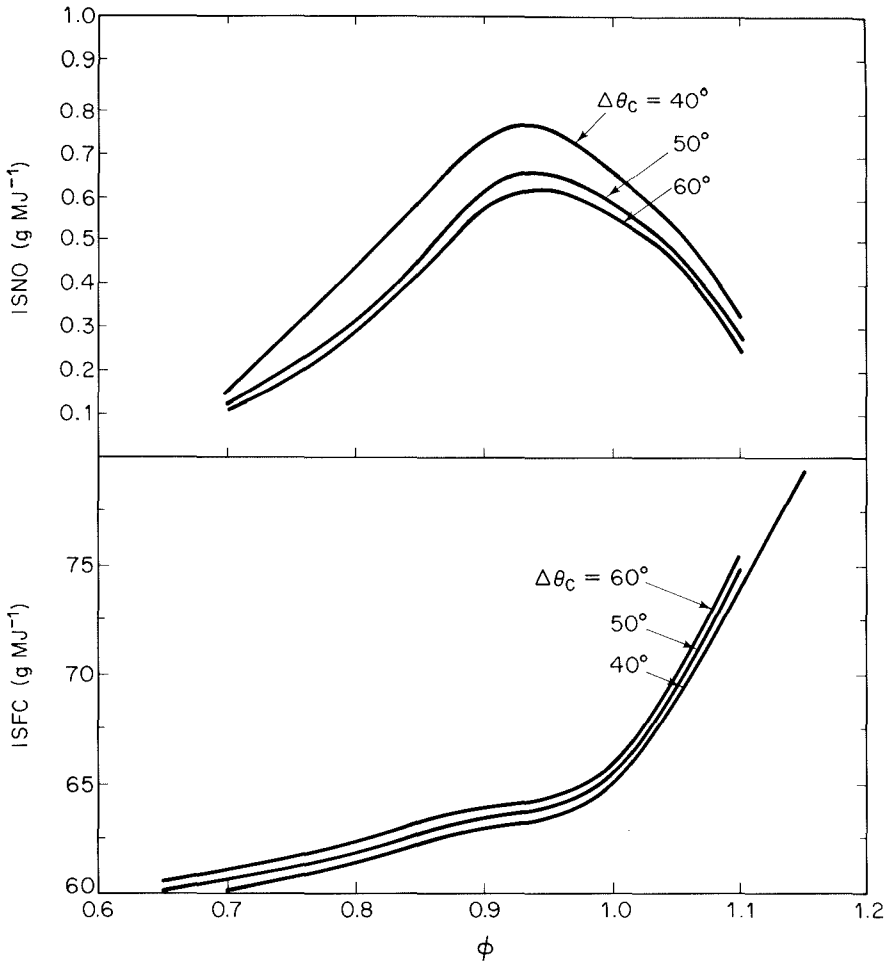


Figure 4.11 Influence of equivalence ratio and combustion duration on NO emissions and fuel consumption (Heywood et al., 1979; © SAE, Inc.).

rapidly as the equivalence ratio is increased or decreased. The fuel consumption increases monotonically with equivalence ratio, with an abrupt change in the rate of increase at $\phi = 1$. The combustion duration influences NO_x emissions more strongly than fuel consumption, but even there the effect is small.

The influence of the operating equivalence ratio on emissions of carbon monoxide and unburned hydrocarbons is illustrated in Figure 4.12. The CO level is relatively low for fuel-lean operation but rises abruptly, as expected, when the mixture becomes fuel-rich. The hydrocarbon emissions, on the other hand, exhibit a minimum and increase for very fuel-lean operation. In lean operation the temperature can be too low for hydrocarbons to burn late in the expansion stroke. Furthermore, the low laminar flame speed at low ϕ means that the flame may not even reach all the mixture.

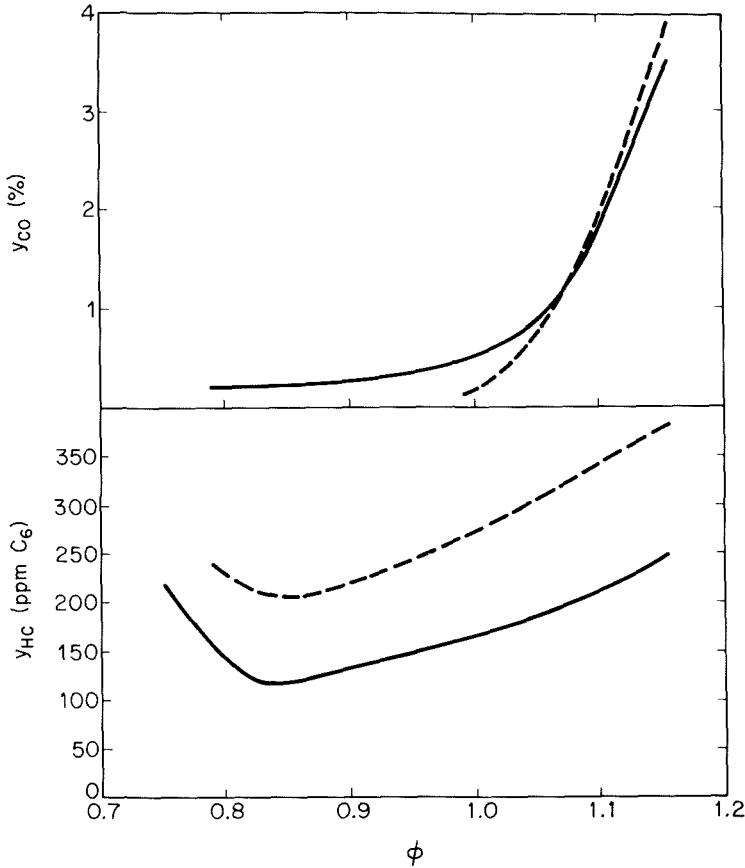


Figure 4.12 Influence of equivalence ratio and load on carbon monoxide and hydrocarbon emissions. Solid lines: 2000 rpm, $\theta_i = -38^\circ$, and 80 km h^{-1} road load; Dashed lines: 1200 rpm, $\theta_i = -10^\circ$, and 48 km h^{-1} road load.

To reduce NO_x emissions significantly, it is necessary to reduce the peak temperature significantly. Delaying the initiation of combustion results in the peak pressure occurring later in the expansion stroke, as illustrated in Figure 4.13. The spark is usually fired before top dead center, so that the combustion rate is maximum near top dead center. Delaying the spark results in the energy release occurring when the cylinder volume has increased significantly. The peak pressure and temperature are therefore reduced by this *spark retard*. At the most extreme level, the spark can be retarded past top dead center so that the gases begin to expand before combustion begins. The influence of equivalence ratio and ignition angle on fuel consumption and NO_x emissions has been calculated by Blumberg and Kummer (1971). Their results are shown in a map of BSFC versus BSNO in Figure 4.14. Clearly, if an engine could be operated at very low equivalence ratios, NO_x emissions could be reduced dramatically with only a minimal efficiency penalty. Operating at equivalence ratios more typical of premixed combustion

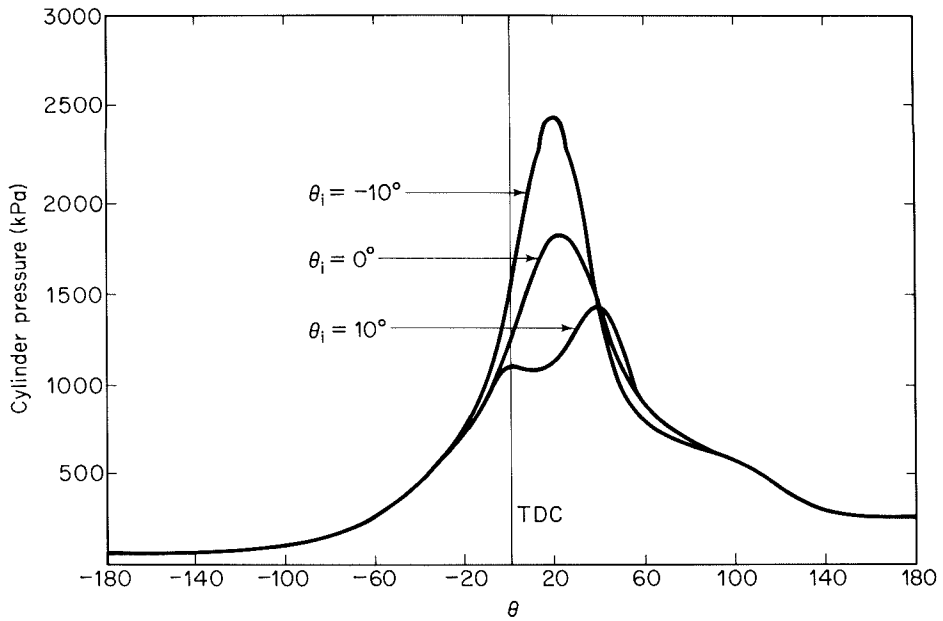


Figure 4.13 Influence of ignition timing on cylinder pressure profiles.

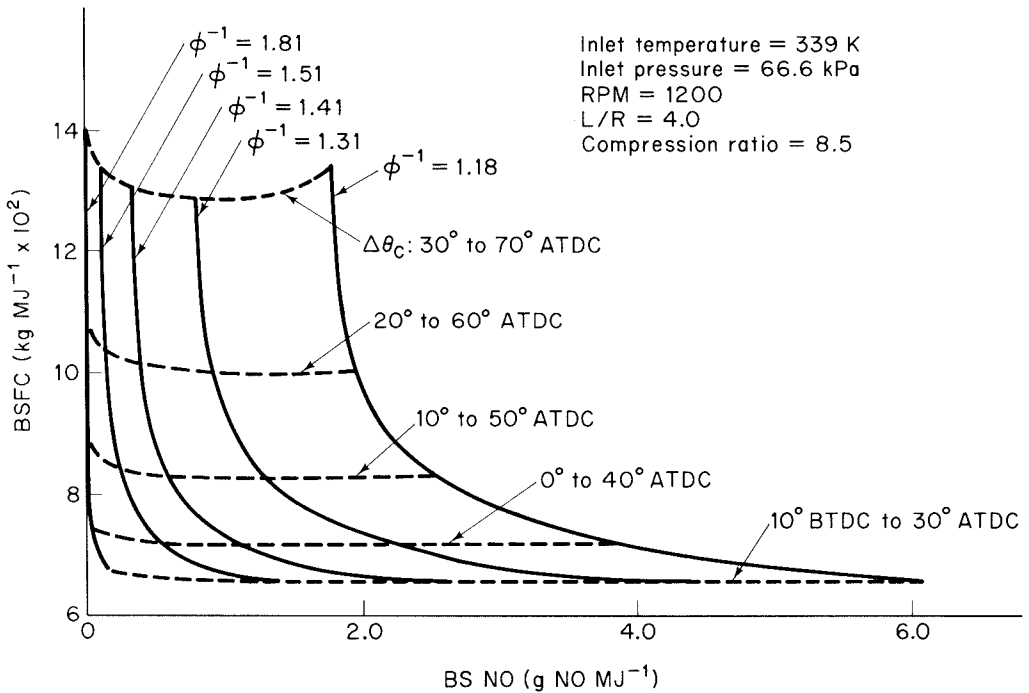


Figure 4.14 Effect of equivalence ratio and ignition timing on efficiency and NO formation for $\Delta\theta_c = 40^\circ$ (Blumberg and Kummer, 1971). Reprinted by permission of Gordon and Breach Science Publishers.

in spark ignition engines and relying on ignition retard to control NO_x yield smaller emission benefits and substantially larger fuel consumption increases. Such emissions/performance trade-offs are typical of efforts to control engine emissions and have been the motivating factor behind much of the research into engine emission control technologies.

Reducing the compression ratio can also lower peak temperatures, thereby limiting NO_x formation. However, the NO_x emission reductions achieved by reducing the compression ratio are small compared to those accrued by retarding the spark.

Another way to reduce the peak temperatures is by diluting the charge with cool combustion products. In engines, this process is called *exhaust gas recirculation (EGR)*. The use of combustion products for dilution instead of excess air has dual benefits:

1. Dilution of the fuel-air mixture without the addition of excess O_2 that aids in NO_x formation.
2. An increase in the specific heat of the gas due to the presence of H_2O and CO_2 . This reduces the temperature somewhat more than would equivalent dilution with excess air.

Figure 4.15 shows how significantly EGR can reduce NO_x emission levels. For small amounts of EGR, the theoretical predictions agree closely with experimental ob-

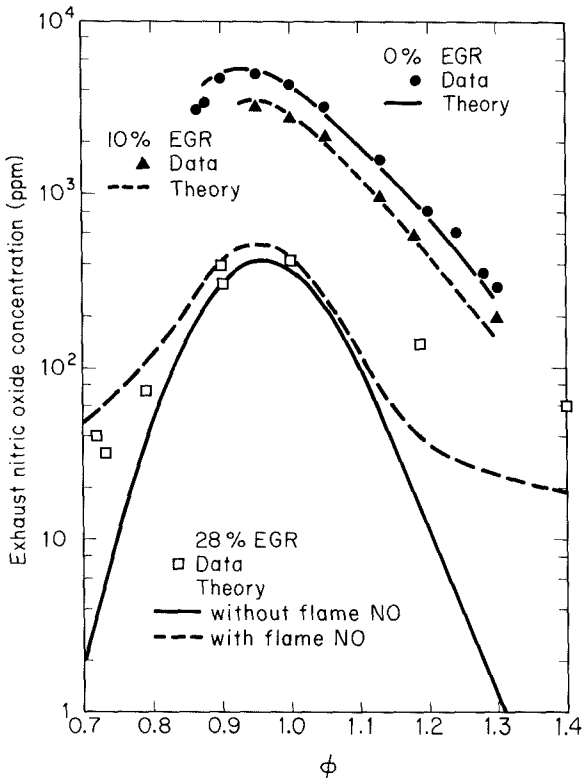


Figure 4.15 Influence of exhaust gas recirculation on NO emissions as a function of equivalence ratio (Heywood, 1975). Reprinted by permission of The Combustion Institute.

servations; however, at 28% EGR, the measured NO_x emission levels for lean or rich mixtures are significantly higher than those predicted considering only postflame chemistry. The dashed curve presents more detailed chemical mechanism calculations that take into account the nonequilibrium radical concentrations that are present within the flame front (i.e., “prompt NO ”). Agreement on the fuel-lean side is very good. On the other hand, even when the flame chemistry of the O, H, and OH radicals is taken into account, the predictions of NO_x formation in fuel-rich combustion are significantly lower than those observed. This discrepancy may be due to nitrogen chemistry not included in the model, particularly the reactions of N_2 with hydrocarbon radicals.

From these results we see the EGR can substantially reduce NO_x formation in spark ignition engines, but the degree of control achievable by this method is limited. These gains are not achieved without penalties. Figure 4.16 shows calculations of the variation of fuel consumption and mean effective pressure with equivalence ratio and amount of exhaust gas recirculated. While the fuel consumption penalty is relatively small, the loss of power is significant, so the engine size must be increased to meet a particular power requirement if EGR is employed to control NO_x emissions.

It is apparent that spark retard and exhaust gas recirculation are effective measures for NO_x emission control. The equivalence ratio range that can be employed effectively is limited. Rich mixtures lead to high CO levels. As the mixture becomes too fuel-lean, hydrocarbon emissions rise. Hence control of emissions without the use of exhaust gas cleaning involves compromises. Spark retard and exhaust gas recirculation are usually used in combination to achieve low NO_x emission levels. The introduction of strict NO_x emission controls in combination with limits on CO and hydrocarbon emissions was accompanied by a substantial increase in fuel consumption of automobiles in the United

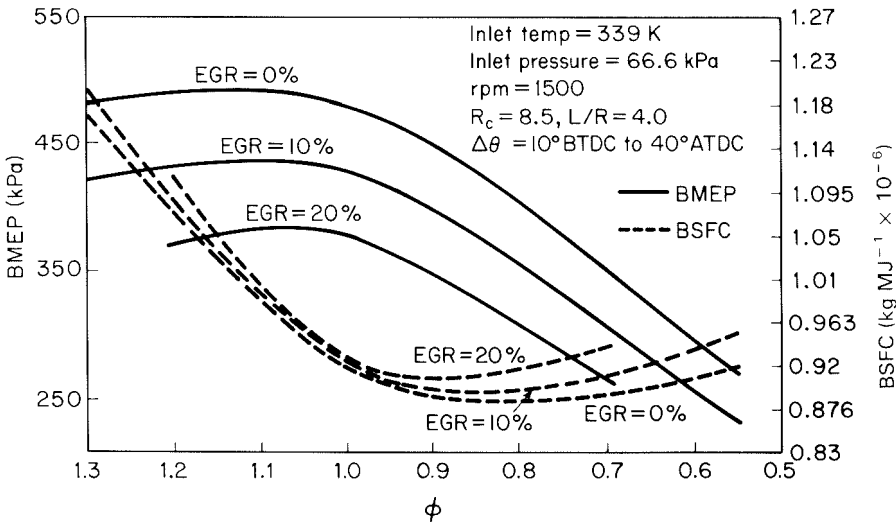


Figure 4.16 Effect of equivalence ratio and exhaust gas recirculation on power (brake mean effective pressure) and fuel consumption (Blumberg and Kummer, 1971). Reprinted by permission of Gordon and Breach Science Publishers.

States. Ultimately, exhaust gas treatment was required to achieve acceptable emissions and performance simultaneously. Exhaust gas treatment is discussed in a subsequent section.

4.1.9 Mixture Preparation

The spark ignition engine burns premixed fuel and air. In conventional engines, this mixture is prepared in the *carburetor*, a complex device that controls both fuel and air flows to the engine. The mixture requirements depend on engine speed and load. A richer mixture is required at high load (such as during vehicle acceleration) than at low load. Even though combustion will be incomplete, fuel-rich mixtures have been used to increase the heat release per cycle, thereby increasing the power delivered by the engine. Carburetors have evolved as mechanically activated control systems that meet these requirements. As we have seen in the preceding discussion, emission controls place additional constraints on engine operation that are not readily met with purely mechanical control. To understand the need for and the nature of the new systems for mixture preparation that are being developed as part of integrated emission control systems, it is useful to examine the operation of a conventional carburetor.

The power output and speed of a spark ignition engine are regulated by a throttle that limits the airflow into the engine. In conventional engines, the airflow rate is used to control the fuel/air ratio. Part of the difficulty encountered in early attempts to reduce automobile emissions derived from the complex coupling of fuel and airflow rates.

A simple carburetor is illustrated in Figure 4.17. The throttle is a butterfly valve, a disk that is rotated to obstruct the airflow, producing a vacuum in the intake manifold. The low pressure reduces the mass entering the cylinders, even though the intake gas volume is fixed. The rate at which fuel is atomized into the airflow is controlled by the pressure drop in a venturi, Δp , that is,

$$G_f = C_{fF} \sqrt{2\rho_f \Delta p_f} \quad (4.41)$$

where G_f is the fuel mass flux, C_{fF} the flow coefficient associated with the fuel metering orifice, ρ_f the density, and Δp_f the pressure drop across the fuel metering orifice. This pressure drop corresponds to the difference between the pressure drop created by the airflow through the venturi Δp_a and the pressure needed to overcome surface tension at the nozzle exit, $\Delta p_\sigma = 2\sigma/d$, where σ is the surface tension and d is the nozzle diameter. The total pressure drop becomes

$$\Delta p_f \approx p_0 + \rho_f gh - p_v - 2\frac{\sigma}{d} \quad (4.42)$$

where p_v is the gas pressure in the venturi. The airflows in the intake system involve large pressure drops, so the compressibility of the gas must be taken into account. The pressure drop associated with the gas flow drives the fuel flow, so we need to know the relationship between pressure drop and flow rate. By considering the conservation of energy, we can readily derive such an expression for the adiabatic and thermodynamically reversible (i.e., isentropic) flow of an ideal gas.

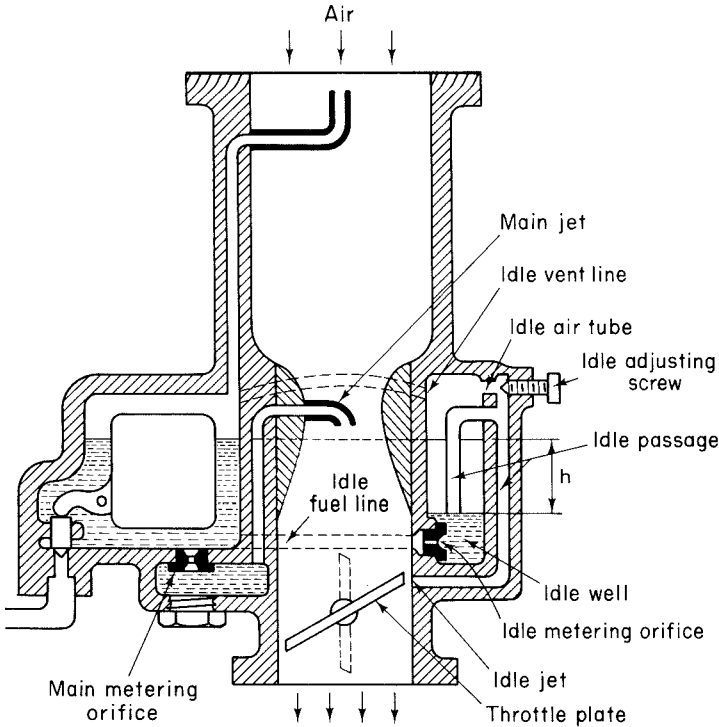


Figure 4.17 Schematic of a simple carburetor.

The flows through real devices such as the venturi or throttle are not perfectly reversible, so the flow rate associated with a given pressure drop is lower than that for isentropic flow. The ratio of the actual flow rate to the ideal flow rate is the flow coefficient for the device, that is,

$$C_f = \frac{G}{G_s} \tag{4.43}$$

where G denotes the mass flux and the subscript s denotes that for isentropic flow. The flow coefficient for a sharp-edged orifice is 0.61. The venturi is designed to achieve nearly reversible flow so that C_f will be closer to unity. The flow coefficient for the throttle changes as the throttle plate is rotated. It is unity when the throttle is fully open and decreases toward that for the orifice as the throttle is closed.

We consider adiabatic flow through the device in question. As the gas is accelerated, its kinetic energy must be taken into account in the fluid energy balance, that is, for the flow at velocities v_1 and v_2 ,

$$\bar{h}_1 + \frac{1}{2} v_1^2 = \bar{h}_2 + \frac{1}{2} v_2^2 = \bar{h}_0$$

h_0 is the stagnation enthalpy corresponding to $v = 0$. Assuming that the gas is ideal and the specific heats are constant, we may write

$$\bar{c}_p(T_0 - T_1) = \frac{1}{2} v_1^2 \quad (4.44)$$

The mass flux is $G = \rho_1 v_1$, so we may write

$$G = \rho \sqrt{2\bar{c}_p(T_0 - T_1)} \quad (4.45)$$

If the flow is adiabatic and isentropic, the density and temperature are related to the pressure by

$$\frac{p}{\rho^\gamma} = \frac{p_0}{\rho_0^\gamma} \quad (4.46)$$

$$\frac{p}{T^{\gamma/\gamma-1}} = \frac{p_0}{T_0^{\gamma/\gamma-1}} \quad (4.47)$$

Using the ideal gas relation and these results, the mass flux thus becomes

$$G_s = p_0 \sqrt{\frac{M}{RT_0}} r^{1/\gamma} \sqrt{\frac{2}{\gamma-1} (1 - r^{(\gamma-1)/\gamma})} \quad (4.48)$$

where $r = p/p_0$ is the pressure ratio.

At sufficiently low pressure ratio, the velocity at the minimum cross-sectional area will equal the local speed of sound (4.3). Further reduction in the pressure below the throat has no influence on the mass flow rate, so the flow is said to be choked. Substituting (4.3) into (4.44), we find

$$\frac{T_0}{T^*} = \frac{\gamma + 1}{2} \quad (4.49)$$

where the asterisk is used to denote a property evaluated at locally sonic conditions. Using (4.47) we find the critical pressure ratio,

$$r^* = \left(\frac{2}{\gamma + 1} \right)^{\gamma/(\gamma-1)} \quad (4.50)$$

The corresponding mass flow rate is obtained by substituting r^* into (4.48),

$$G_s(r^*) = p_0 \sqrt{\frac{M}{RT_0}} \left(\frac{2}{\gamma + 1} \right)^{(\gamma+1)/2(\gamma-1)} \quad (4.51)$$

The mass flow rate for a real device becomes

$$G_f \approx C_f p_0 \sqrt{\frac{M}{RT_0}} r^{1/\gamma} \sqrt{\frac{2}{\gamma-1} (1 - r^{(\gamma-1)/\gamma})} \quad r > r^* \quad (4.52)$$

$$G_f \approx C_f p_0 \sqrt{\frac{M}{RT_0}} \left(\frac{2}{\gamma + 1} \right)^{(\gamma+1)/2(\gamma-1)} \quad r \leq r^*$$

For a well-designed venturi, the flow coefficient will be nearly unity and the stagnation pressure downstream of the venturi will be close to that at the venturi inlet. Butterfly valves and other nonideal flow devices will have lower flow coefficients. If a subsonic flow separates at the minimum area, the pressure at that point will correspond approximately to the downstream stagnation pressure. Thus, closing the throttle results in the pressure in the intake manifold being substantially below atmospheric pressure.

The fuel flow rate is governed by the pressure at the throat of the venturi, so (4.41) can be expressed in terms of the pressure ratio

$$G_f = C_{fF} \sqrt{2\rho_f \left[p_0(1 - r) + gz - \frac{2\sigma}{d} \right]} \tag{4.53}$$

The fuel/air ratio becomes (for $r > r^*$)

$$\frac{G_f A_f}{G_a A_a} = \frac{A_f C_{fF} \sqrt{2\rho_f \left[p_0(1 - r) + gz - \frac{2\sigma}{d} \right]}}{A_a C_{fF} p_0 \sqrt{\frac{M}{RT_0}} r^{1/\gamma} \sqrt{\frac{2}{\gamma - 1} (1 - r^{(\gamma-1)/\gamma})}} \tag{4.54}$$

The complex dependence of the equivalence ratio on the pressure ratio is readily apparent.

Examining (4.42) we see that, for

$$r \geq 1 - \frac{2\sigma}{p_0 d} + \frac{gz}{p_0} \tag{4.55}$$

the pressure drop in the venturi is insufficient to overcome surface tension and atomize the fuel. These high pressure ratios (low pressure drops) correspond to low engine speeds. A separate idle nozzle supplies the fuel necessary for low-speed operation. This ideal adjustment is coupled to the pressure drop at the throttle valve.

Figure 4.18 illustrates the variation of equivalence ratio with airflow that is produced by these metering devices. The pressure in the venturi throat decreases with increasing airflow. Since the difference between this pressure and that of the atmosphere provides the driving force for the main fuel flow, the fuel supplied by the main jet increases with increasing airflow. The idle jet compensates for the precipitous drop in the fuel flow supplied by the main jet. The pressure at the throttle plate provides the driving force for the idle fuel flow, so this flow is significant only when the idle plate is closed, i.e., at low airflow. As the throttle plate is opened and the airflow increases, the idle fuel flow decreases markedly. The operating equivalence ratio of the engine is determined by the sum of the two fuel flows, shown by the upper curve.

At high engine load, a richer mixture may be required than is supplied by this simple metering system. The power jet shown in Figure 4.19 is one method used to supply the additional fuel. Ideally, the throttle position at which the power jet opens would vary with engine speed. A mechanical linkage that opens gradually as the throttle

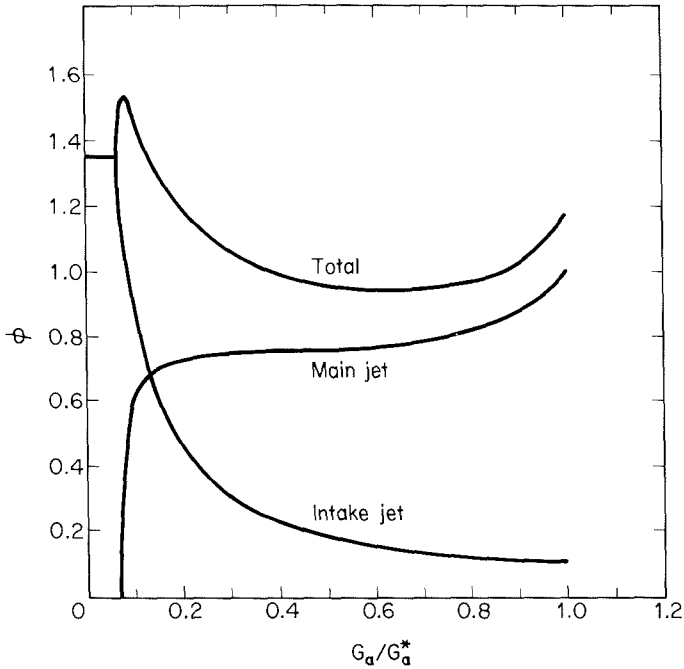


Figure 4.18 Variation of equivalence ratio with airflow rate for a simple carburetor (Taylor, 1966). Reprinted by permission of MIT Press.

opens beyond some point is a compromise solution. When the power jet is fully open, the fuel flow is about 10% more than that supplied by the main jet.

If the throttle is rapidly opened (as when the gas pedal of a car is quickly depressed), the fuel flow does not respond instantly. To improve the engine response, an accelerator pump may be used to supply fuel at a rate that is proportional to the speed of the accelerator motion.

A very fuel-rich mixture is used to start a cold engine, on the assumption that if enough fuel is introduced into the intake manifold, some of it will surely evaporate and start the engine. A butterfly valve called a *choke* is installed between the impact tube and the venturi, as illustrated in Figure 4.19, to increase the pressure drop and therefore the fuel flow rate through the main metering orifice. The choke is frequently operated automatically, controlled by the exhaust manifold temperature and the inlet manifold pressure. Rich operation during startup leads to high CO and hydrocarbon emissions. As much as 40% of the hydrocarbons emitted during automotive test cycles may be released during the warm-up phase.

We have examined only a few of the features that have been incorporated into automotive carburetors. Since the carburetor directly controls the equivalence ratio of the mixture reaching the engine, it plays a central role in the control of automotive emissions. Much more elaborate fuel metering systems have been developed to achieve

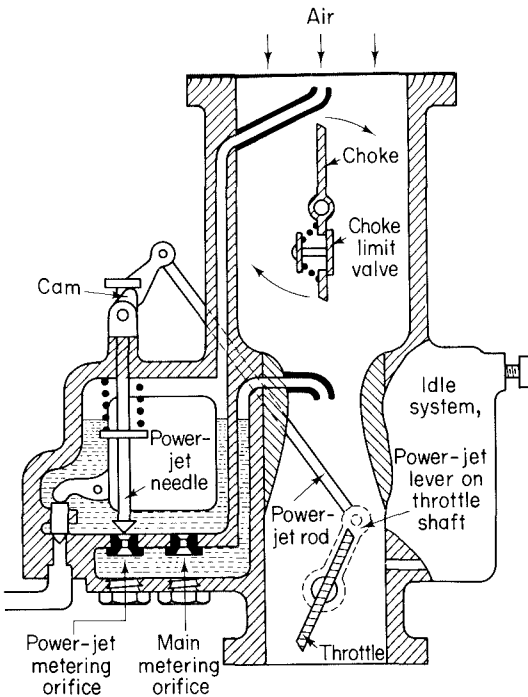


Figure 4.19 Carburetor with power jet and choke (Taylor, 1966). Reprinted by permission of MIT Press.

the fine regulation required for emission control. Electronically manipulated valves have replaced the simple mechanically controlled fuel metering, facilitating more precise control of engine operation through the use of computers.

Fuel injection is used in place of carburetion in some spark ignition engines because the quantity of fuel introduced can be controlled independently of the airflow rate. Atomization of high-pressure fuel replaces the flow-induced fuel intake of conventional carburetors. Fuel may be injected into the intake manifold (injection carburetion) so that the mixture is controlled by an injector pump rather than being directly coupled to the airflow. Injection into the inlet ports allows cylinder-by-cylinder regulation of the equivalence ratio. Direct injection into the cylinder is also used in some engines, although this method is more sensitive to spray characteristics and may lead to imperfect mixing of fuel and air. Injection systems are becoming more common because they are so well suited to integration into feedback-controlled engine operation.

4.1.10 Intake and Exhaust Processes

The flows through the intake and exhaust valves also influence engine operation and emissions. We have seen that the intake flow induces turbulence that, after amplification by rapid compression, governs the flame propagation. The opening of the exhaust valve near the end of the expansion stroke causes a sudden pressure decrease and adiabatic cooling that influence carbon monoxide emissions.

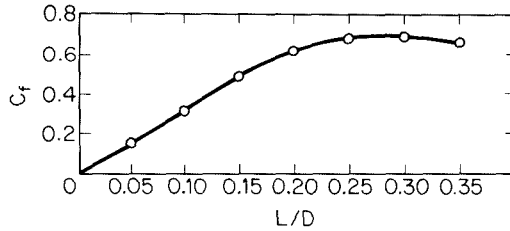
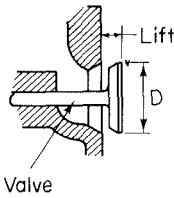


Figure 4.20 Poppet valve geometry and flow coefficient (Taylor, 1966). Reprinted by permission of MIT Press.

The poppet valves through which the charge enters and the combustion products exit from the cylinder are illustrated in Figure 4.20. The mass fluxes through these valves are also described by the compressible flow relation, (4.53). The discharge coefficient depends on the valve lift, L , as illustrated in Figure 4.20. For large lift, $L/D > 0.25$, the flow coefficient based on the valve area approaches a constant value of about 0.65, slightly larger than that for a sharp-edged orifice. For smaller lift, the flow coefficient is proportional to the lift, suggesting the area of a cylinder between the valve and the port could be used to describe the flow with a constant coefficient. Shrouds placed on the intake valve to induce swirl or to increase engine turbulence reduce the open area on this cylinder and therefore the flow rate.

The intake and exhaust flows are not steady. There may be a substantial pressure difference between the cylinder and the manifold when a valve is first opened, leading to a brief period of very high flow rate. This transient flow is particularly pronounced during exhaust when the flow is initially choked. After a brief *blowdown*, the pressure drop decreases and the flow rate is governed by the piston motion. Calculated and measured flow rates from the work of Tabaczynski et al. (1972) are presented in Figure 4.9. Note that the exhaust valve opens about 50° before bottom dead center to allow the cylinder pressure to drop before the beginning of the exhaust stroke. It is also common practice to open the intake valve before the end of the exhaust stroke. This overlap reduces the amount of residual combustion products being mixed with the fresh charge. Improved scavenging achieved in this way increases the engine power output.

The exhaust system includes a length of pipe, a muffler, and gas-cleaning equipment through which the combustion products must flow before entering the atmosphere. The pressure in the exhaust manifold must therefore be greater than atmospheric pressure. The pressure of the gas entering the cylinder is lower than atmospheric pressure, due to pressure drops in the carburetor (particularly across the throttle), intake manifold, and inlet valve. The work required to draw the fuel and air into the cylinder and to pump the combustion products from the cylinder is called the *pumping work*.

The pressure in the cylinder at the end of the intake stroke only approaches atmospheric pressure for open-throttle operation at relatively low speed. From the cycle analysis, it should be apparent that the peak pressure and temperature depend on the intake pressure. Heat transfer from the hot engine block to the fuel-air mixture also influences the temperature. The variation of temperature and pressure with throttle po-

sition, engine speed, and engine temperature can be expected to be important factors in the formation of pollutants.

4.1.11 Crankcase Emissions

Crankcase emissions are caused by the escape of gases from the cylinder during the compression and power strokes. The gases escape between the sealing surfaces of the piston and cylinder wall into the crankcase. This leakage around the piston rings is commonly called *blowby*. Emissions increase with increasing engine airflow, that is, under heavy load conditions. The resulting gases emitted from the crankcase consist of a mixture of approximately 85% unburned fuel–air charge and 15% exhaust products. Because these gases are primarily the carbureted fuel–air mixture, hydrocarbons are the main pollutants. Hydrocarbon concentrations in blowby gases range from 6000 to 15,000 ppm. Blowby emissions increase with engine wear as the seal between the piston and cylinder wall becomes less effective. On cars without emission controls, blowby gases are vented to the atmosphere by a draft tube and account for about 25% of the hydrocarbon emissions.

Blowby was the first source of automotive emissions to be controlled. Beginning with 1963 model cars, this category of vehicular emissions has been controlled in cars made in the United States. The control is accomplished by recycling the blowby gas from the crankcase into the engine air intake to be burned in the cylinders, thereby keeping the blowby gases from escaping into the atmosphere. All control systems use essentially the same approach, which involves recycling the blowby gases from the engine oil sump to the air intake system. A typical system is shown in Figure 4.21. Ventilation air is drawn down into the crankcase and then up through a ventilator valve and hose and into the intake manifold. When airflow through the carburetor is high, additional air from the crankcase ventilation system has little effect on engine operation. However, during idling, airflow through the carburetor is so low that the returned blowby gases could alter the air–fuel ratio and cause rough idling. For this reason, the flow control valve restricts the ventilation flow at high intake manifold vacuum (low engine speed) and permits free flow at low manifold vacuum (high engine speed). Thus high ventilation rates occur in conjunction with the large volume of blowby associated with high speeds; low ventilation rates occur with low-speed operation. Generally, this principle of controlling blowby emissions is called *positive crankcase ventilation* (PCV).

4.1.12 Evaporative Emissions

Evaporative emissions issue from the fuel tank and the carburetor. Fuel tank losses result from the evaporation of fuel and the displacement of vapors when fuel is added to the tank. The amount of evaporation depends on the composition of the fuel and its temperature. Obviously, evaporative losses will be high if the fuel tank is exposed to high ambient temperatures for a prolonged period of time. The quantity of vapor expelled when fuel is added to the tank is equal to the volume of the fuel added.

Evaporation of fuel from the carburetor occurs primarily during the period just

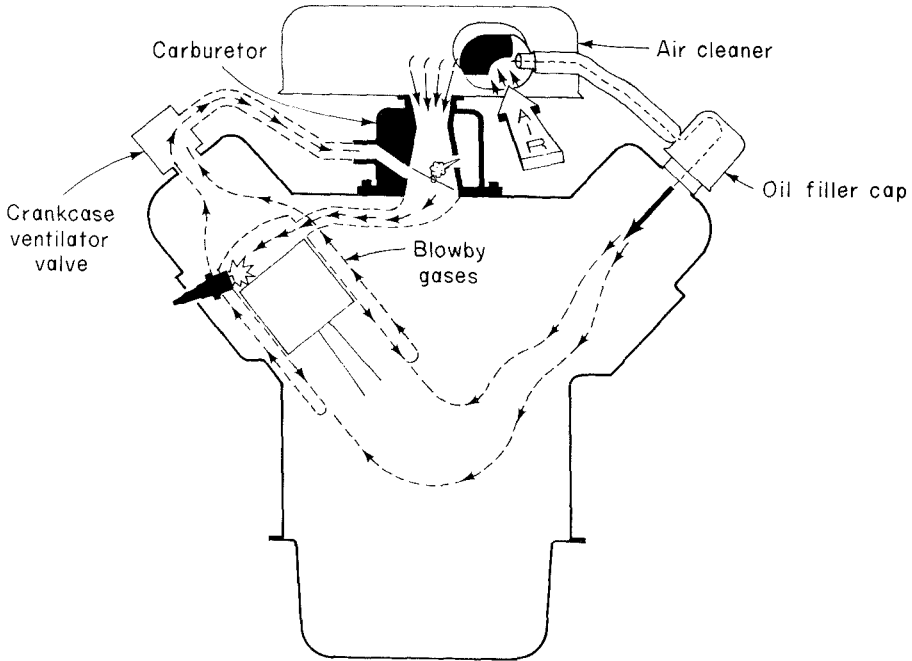


Figure 4.21 Crankcase emission control system.

after the engine is turned off. During operation the carburetor and the fuel in the carburetor remain at about the temperature of the air under the hood. But the airflow ceases when the engine is stopped, and the carburetor bowl absorbs heat from the hot engine, causing fuel temperatures to reach 293 to 313 K above ambient and causing gasoline to vaporize. This condition is called a *hot soak*. The amount and composition of the vapors depend on the fuel volatility, volume of the bowl, and temperature of the engine prior to shutdown. On the order of 10 g of hydrocarbons may be vaporized during a hot soak. Fuel evaporation from both the fuel tank and the carburetor accounts for approximately 20% of the hydrocarbon emissions from an uncontrolled automobile.

It is clear that gasoline volatility is a primary factor in evaporative losses. The measure of fuel volatility is the empirically determined *Reid vapor pressure*, which is a composite value reflecting the cumulative effect of the individual vapor pressures of the different gasoline constituents. It provides both a measure of how readily a fuel can be vaporized to provide a combustible mixture at low temperatures and an indicator of the tendency of the fuel to vaporize. In a complex mixture of hydrocarbons, such as gasoline, the lowest-molecular-weight molecules have the greatest tendency to vaporize and thus contribute more to the overall vapor pressure than do the higher-molecular-weight constituents. As the fuel is depleted of low-molecular-weight constituents by evaporation, the fuel vapor pressure decreases. The measured vapor pressure of gasoline therefore depends on the extent of vaporization during the test. The Reid vapor-pressure determination is a standard test at 311 K in which the final ratio of vapor volume to

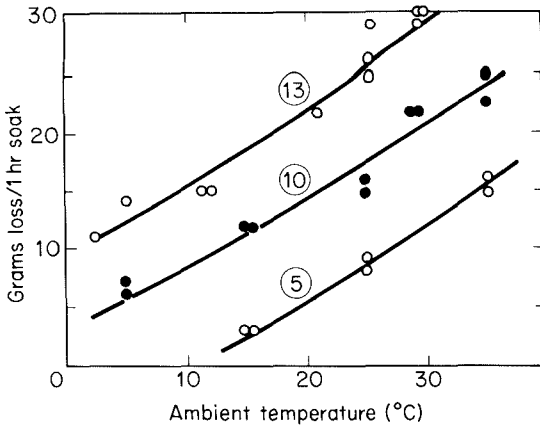


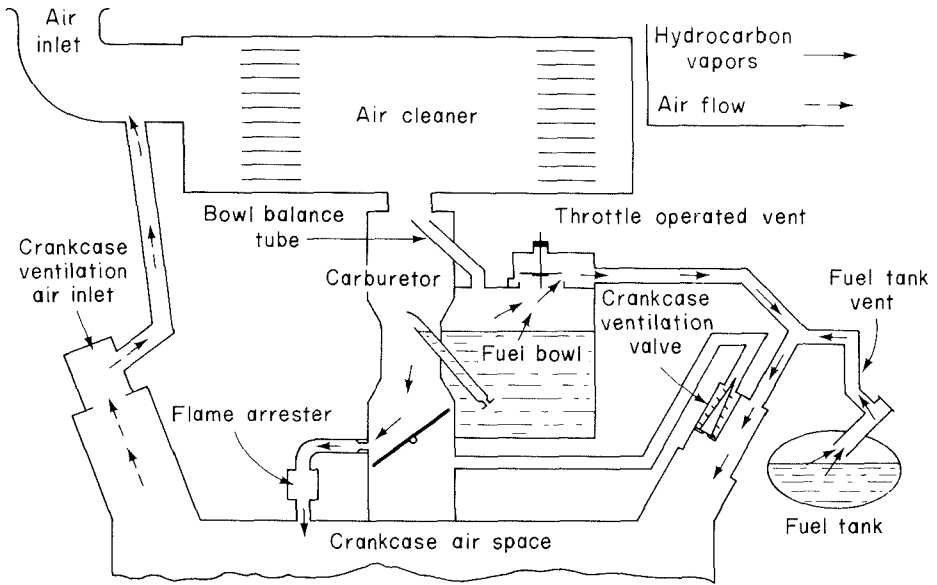
Figure 4.22 Variation of evaporation loss from an uncontrolled carburetor with fuel vapor pressure and temperature. Numbers in large circles are Reid vapor pressure.

liquid volume is constant (4:1) so that the extent of vaporization is always the same. Therefore, the Reid vapor pressure for various fuels can be used as a comparative measure of fuel volatility.

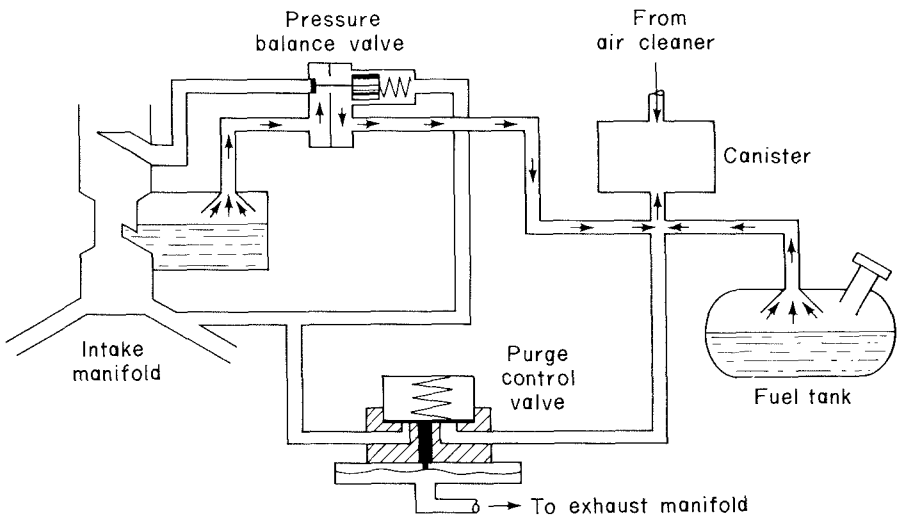
Figure 4.22 shows carburetor evaporative loss as a function of temperature and Reid vapor pressure. The volatility and thus the evaporative loss increase with Reid vapor pressure. In principle, evaporative emissions can be reduced by reducing gasoline volatility. However, a decrease in fuel volatility below the 8 to 12 Reid vapor pressure range, commonly used in temperate climates, would necessitate modifications in carburetor and intake manifold design, required when low vapor pressure fuel is burned. In view of costly carburetion changes associated with reduction of fuel volatility, evaporative emission control techniques have been based on mechanical design changes. Two evaporative emission control methods are the *vapor-recovery system* and the *adsorption-regeneration system*.

In the vapor-recovery system, the crankcase is used as a storage tank for vapors from the fuel tank and carburetor. Figure 4.23(a) shows the routes of hydrocarbon vapors during shutdown and hot soak. During the hot-soak period the declining temperature in the crankcase causes a reduction in crankcase pressure sufficient to draw in vapors. During the hot soak, vapors from the carburetor are drawn into the crankcase. Vapor from the fuel tank is first carried to a condenser and vapor-liquid separator, with the vapor then being sent to the crankcase and the condensate to the fuel tank. When the engine is started, the vapors stored in the crankcase are sent to the air intake system by the positive crankcase ventilation system.

In the adsorption-regeneration system, a canister of activated charcoal collects the vapors and retains them until they can be fed back into the intake manifold to be burned. The system is shown in Figure 4.23(b). The essential elements of the system are the canister, a pressure-balancing valve, and a purge control valve. During the hot-soak period, hydrocarbon vapors from the carburetor are routed by the pressure balance valve to the canister. Vapor from the fuel tank is sent to a condenser and separator, with liquid fuel returned to the tank. When the engine is started, the pressure control valve causes



(a)



(b)

Figure 4.23 Evaporative emission control systems: (a) use of crankcase air space: (b) adsorption-regeneration system.

air to be drawn through the canister, carrying the trapped hydrocarbons to the intake manifold to be burned.

4.1.13 Exhaust Gas Treatment

Modification of engine operation yields only modest emission reductions, and the penalties in engine performance and efficiency are substantial. An alternative way to control emissions involves the treatment of the exhaust gas in chemical reactors. Carbon monoxide, unburned hydrocarbons, and nitrogen oxides are all present in the exhaust gases in concentrations that are far in excess of the equilibrium values. If all the pollutants are to be controlled by exhaust gas treatment, it is necessary to *oxidize* carbon monoxide and hydrocarbons while *reducing* nitrogen oxides. Exhaust gas treatment may utilize either catalytic converters or noncatalytic thermal reactors.

Thermal reactors. The gas-phase oxidation of carbon monoxide slows dramatically as combustion products cool, but the reaction does not stop entirely. In fact, carbon monoxide and hydrocarbons continue to react in the exhaust manifold. To oxidize the hydrocarbons homogeneously requires a holding time of order 50 ms at temperatures in excess of 900 K. Homogeneous oxidation of carbon monoxide requires higher temperatures, in excess of 1000 K. The oxidation rate can be enhanced with a thermal reactor—an enlarged exhaust manifold that bolts directly onto the cylinder head. The thermal reactor increases the residence time of the combustion products at temperatures sufficiently high that oxidation reactions can proceed at an appreciable rate. To allow for fuel-rich operation, secondary air may be added and mixed rapidly with combustion products.

A multiple-pass arrangement is commonly used in thermal reactors to shield the hot core of the reactor from the relatively cold surroundings. This is critical since the reactions require nearly adiabatic operation to achieve significant conversion, as illustrated in Figure 4.24. Typically, only about a factor of 2 reduction in emission levels for CO and hydrocarbons can be achieved even with adiabatic operation. Higher temperatures and long residence times are typically required to achieve better conversions. The heat released in the oxidation reactions can result in a substantial temperature rise and, thereby, promote increased conversion. Removal of 1.5% CO results in a temperature rise of about 490 K (Heywood, 1976). Hence thermal reactors with fuel-rich cylinder exhaust gas and secondary air addition give greater fractional reductions in CO and hydrocarbon levels than reactors with fuel-lean cylinder exhaust. Incomplete combustion in the cylinder, however, does result in reduced fuel economy. The attainable conversion is limited by incomplete mixing of gases exhausted at various times in the cycle and any secondary air that is added.

Temperatures of the exhaust gases of automobile spark ignition engines can vary from 600 to 700 K at idle to 1200 K during high-power operation. Most of the time the exhaust temperature is between 700 and 900 K, too low for effective homogeneous oxidation. Spark retard increases the exhaust temperature, but this is accompanied by a significant loss in efficiency.

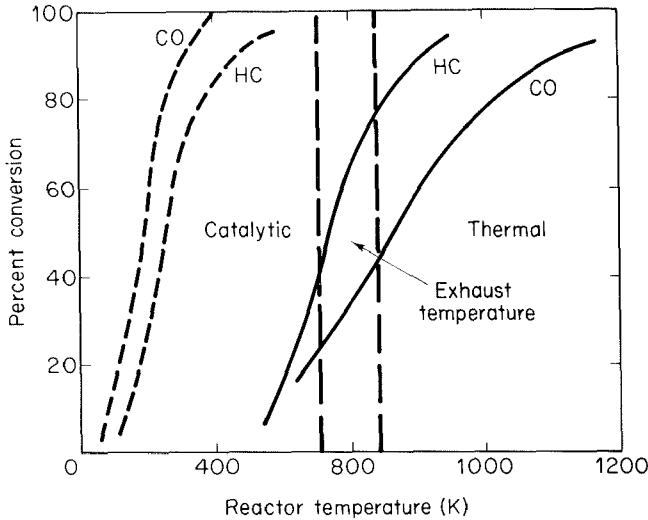


Figure 4.24 Comparison of catalytic converter and thermal reactor for oxidation of CO and hydrocarbons.

Noncatalytic processes for vehicular emission control can yield significant improvements in carbon monoxide and hydrocarbon emissions. The problem of NO_x emission control is not easily alleviated with such systems. Control of NO_x emissions through noncatalytic reduction by ammonia is feasible only in a very narrow window of temperature, toward the upper limit of the normal exhaust temperature range, making joint control of products of incomplete combustion and NO_x a severe technological challenge. Furthermore, the need to ensure a proper flow of ammonia presents a formidable logistical problem in the implementation of such technologies for control of vehicular emissions.

Catalytic converters. By the use of oxidation catalysts, the oxidation of carbon monoxide and hydrocarbon vapors can be promoted at much lower temperatures than is possible in the gas phase, as shown in Figure 4.24. The reduction of NO is also possible in catalytic converters, provided that the oxygen content of the combustion products is kept sufficiently low. In the catalytic converter, the exhaust gases are passed through a bed that contains a small amount of an active material such as a noble metal or a base metal oxide deposited on a thermally stable support material such as alumina. Alumina, by virtue of its porous structure, has a tremendous surface area per unit volume. Small pellets, typically a few millimeters in diameter, or thin-walled, honeycomb, monolithic structures, illustrated in Figure 4.25, are most commonly used as the support. Pellet supports are inexpensive, but when packed closely in a reactor, they produce large pressure drops across the device, increasing the back-pressure in the exhaust system. They may suffer from attrition of the catalyst pellets due to motion during use. This problem can be reduced, but not entirely overcome, through the use of hard, relatively high density pellets. The mass of the catalyst bed, however, increases the time required for the bed to heat to the temperature at which it becomes catalytically active, thereby allowing substantial CO and hydrocarbon emissions when the engine is first started. Mon-

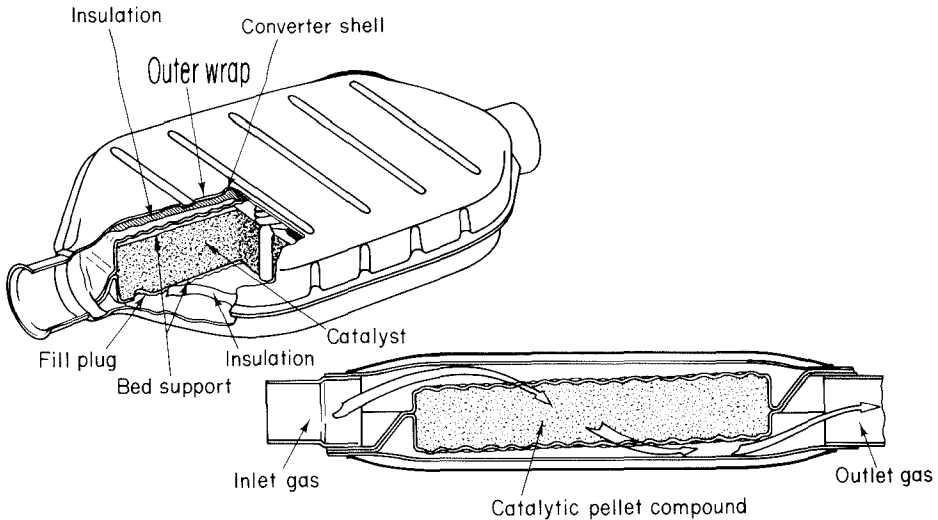


Figure 4.25 Schematic of pellet-type catalytic converter.

olitic supports allow a freer exhaust gas flow, but are expensive and less resistant to mechanical and thermal damage. In particular, the rapid temperature changes to which a vehicular catalytic converter is exposed make thermal shock a very serious problem.

Many materials will catalyze the oxidation of CO or hydrocarbons at typical exhaust gas temperatures. The oxidation activities per unit surface area for noble metals, such as platinum, are high for both CO and hydrocarbons. Base metal oxide catalysts, notably CuO and Co_3O_4 , exhibit similar activities for CO oxidation but are significantly less active for hydrocarbon oxidation (Kummer, 1980). Base metal catalysts degrade more rapidly at high temperature than do the noble metal catalysts. They are also more susceptible to poisoning by trace contaminants in fuels, such as sulfur, lead, or phosphorus. Hence most automotive emission catalysts employ noble metals.

NO reduction can be achieved catalytically if the concentrations of reducing species are present in sufficient excess over oxidizing species. CO levels in the exhaust gases of 1.5 to 3% are generally sufficient.

Two schemes are employed to achieve catalytic control of both NO_x and products of incomplete combustion: (1) dual-bed catalytic converters and (2) three-way catalysts. The dual-bed system involves operation of the engine fuel-rich, to promote the reduction of NO_x . Secondary air is then added to facilitate the oxidation of CO and hydrocarbons in a second catalyst. Rich operation, while necessary for the NO reduction, results in reduced engine efficiency. Furthermore, it imposes severe restrictions on engine operation. If the exhaust gases are too rich, some of the NO may be converted to NH_3 or HCN. The oxidation catalyst used to eliminate CO and hydrocarbons readily oxidizes these species back to NO, particularly if the catalyst temperature exceeds 700 K.

If the engine is operated at all times at equivalence ratios very close to unity, it is possible to reduce NO and oxidize CO and hydrocarbons on a single catalyst bed known as a *three-way catalyst* (Kummer, 1980). The three-way catalytic converter requires very

precise control of the operating fuel/air ratio of the engine to ensure that the exhaust gases remain in the narrow composition window illustrated in Figure 4.26.

Platinum can be used to reduce NO_x , but the formation of NH_3 under fuel-rich conditions limits its effectiveness as an NO_x -reducing catalyst. NO can be reduced in slightly fuel-lean combustion products if a rhodium catalyst is used. Moreover, rhodium does not produce NH_3 efficiently under fuel-rich conditions. Rhodium is not effective, however, for the oxidation of paraffinic hydrocarbons. In fuel-lean mixtures, platinum is an effective oxidation catalyst. To achieve efficient control of CO and hydrocarbons during the fuel-rich excursions, a source of oxygen is needed. Additives that undergo reduction and oxidation as the mixture composition cycles from fuel-lean to fuel-rich and back (e.g., ReO_2 or CeO_2), may be added to the catalyst to serve as an oxygen reservoir. Three-way catalysts are thus a mixture of components designed to facilitate the simultaneous reduction of NO_x and oxidation of CO and hydrocarbons.

Because this technology allows engine operation near stoichiometric where the efficiency is greatest, and because the advent of semiconductor exhaust gas sensors and microcomputers make feedback control of the fuel-air mixture feasible, the three-way converter has rapidly become the dominant form of exhaust gas treatment in the United States. The extremely narrow operating window has been a major driving force behind

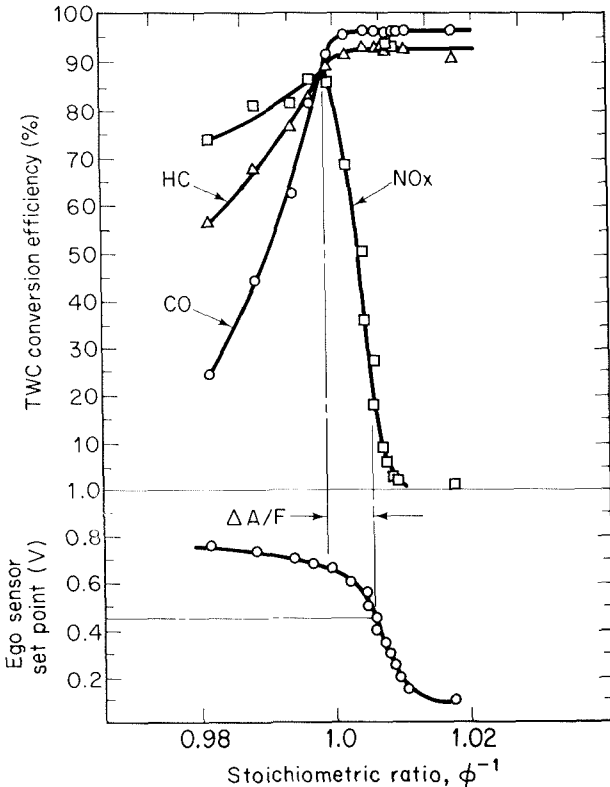


Figure 4.26 Three-way catalyst conversion efficiency and exhaust gas oxygen sensor signal as a function of equivalence ratio (Hamburg et al., 1983; © SAE, Inc.).

the replacement of mechanically coupled carburetors with systems better suited to electronic control.

Feedback control of engines using exhaust gas sensors results in operation that oscillates about the stoichiometric condition in a somewhat periodic manner (Kummer, 1980). The frequency of these oscillations is typically on the order of 0.5 to 4 Hz, with excursions in equivalence ratio on the order of ± 0.01 equivalence ratio units.

In addition to NO, CO, and unoxidized hydrocarbons, catalyst-equipped spark ignition engines can emit sulfuric acid aerosol, aldehydes, and under rich conditions, H₂S. Unleaded gasoline typically contains 150 to 600 ppm by weight of sulfur. The sulfur leaves the cylinder as SO₂, but the catalyst can promote further oxidation to SO₃. As the combustion products cool, the SO₃ combines with water to form an H₂SO₄ aerosol. H₂S formation requires high catalyst temperatures (> 875 K) and a reducing atmosphere. This may occur, for example, when an engine is operated steadily at high speed for some time under fuel-lean conditions and is then quickly slowed to idle fuel-rich operation. HCN formation may occur under similar conditions.

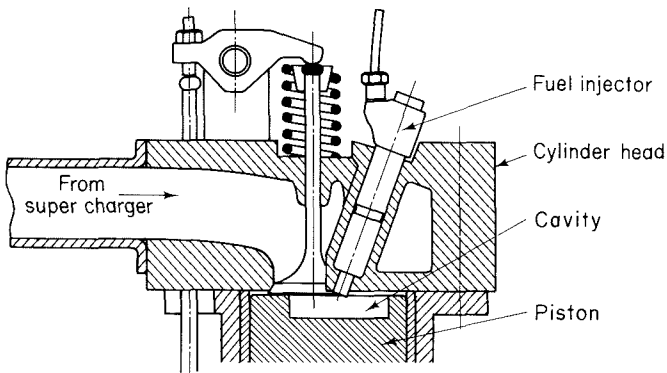
During startup, when the catalyst is cold, hydrocarbons may be only partially oxidized, leading to the emission of oxygenated hydrocarbons. Aldehyde emissions, however, are generally low when the catalyst is hot.

4.2 DIESEL ENGINE

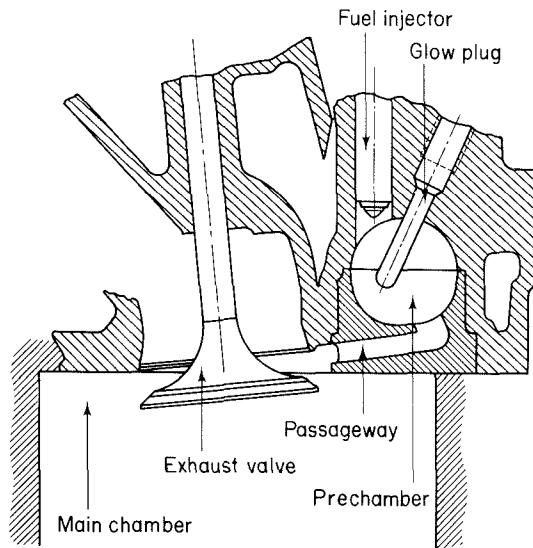
Like the spark ignition engine, the diesel is a reciprocating engine. There is, however, no carburetor on the diesel. Only air (and possibly recycled combustion products for NO_x control by EGR) is drawn into the cylinder through the intake valve. Fuel is injected directly into the cylinder of the diesel engine, beginning toward the end of the compression stroke. As the compression heated air mixes with the fuel spray, the fuel evaporates and ignites. Relatively high pressures are required to achieve reliable ignition. Excessive peak pressures are avoided by injecting the fuel gradually, continuing far into the expansion stroke.

The rate at which the fuel is injected and mixes with the air in the cylinder determines the rate of combustion. This injection eliminates the need to throttle the airflow into the engine and contributes to the high fuel efficiency of the diesel engine. As in the steady-flow combustor, turbulent mixing profoundly influences the combustion process and pollutant formation. The unsteady nature of combustion in the diesel engine significantly complicates the process. Rather than attempt to develop quantitative models of diesel emissions, we shall explore some of the features that govern the formation of pollutants in diesel engines.

Several diesel engine configurations are in use today. Fuel is injected directly into the cylinder of the direct injection (DI) diesel, illustrated in Figure 4.27(a). In the direct injection diesel engine, most of the turbulence is generated prior to combustion by the airflow through the intake valve and the displacement of gases during the compression stroke. The fuel jet is turbulent, but the time scale for mixing is comparable to that for entrainment, so the gas composition does not approach homogeneity within the fuel jet.



(a)



(b)

Figure 4.27 Diesel engine types: (a) direct injection; (b) prechamber.

The use of a prechamber, as shown in Figure 4.27(b), enhances the mixing of the fuel and air in the indirect injection (IDI) or prechamber diesel engine. As the gases burn within the prechamber, they expand through an orifice into the main cylinder. The high kinetic energy of the hot gas jet is dissipated as turbulence in the jet and cylinder. This turbulence enhances mixing over that of the direct injection engine. Improved mixing limits the amount of very fuel-rich gas in the cylinder, thereby reducing soot emissions. Most light-duty diesel engines are of the indirect injection type because of the reduced particulate emissions afforded by this technology. This benefit is not without costs, how-

ever. The flow through the orifice connecting the prechamber to the cylinder results in a pressure drop, thereby reducing the efficiency of the engine.

Diesel engines may also be classified into naturally aspirated (NA), supercharged, or turbocharged types, depending on the way the air is introduced into the cylinder. In the naturally aspirated engine, the air is drawn into the cylinder by the piston motion alone. The supercharger is a mechanically driven compressor that increases the airflow into the cylinder. The turbocharger similarly enhances the intake airflow by passing the hot combustion products through a turbine to drive a centrifugal (turbine-type) compressor.

Compression of the air prior to introduction into the cylinder results in compression heating. This may be detrimental from the point of view of NO_x formation because it increases the peak combustion temperature. An intercooler may be installed between the compressor and the intake valve to reduce this heating.

The fuel is sprayed into the cylinder through a number of small nozzles at very high pressure. The liquid stream issuing from the injector nozzle moves with high velocity relative to the gas. The liquid stream forms filaments that break into large droplets. The breakup of the droplets in the fuel spray is characterized by the Weber number, the ratio of the inertial body forces to surface tension forces,

$$\text{We} = \frac{\rho_g D v^2}{\sigma}$$

where ρ_g is the gas density, v the relative velocity between the gas and the droplets, and σ the surface tension of the liquid. As long as the Weber number exceeds a critical value of approximately 10, the droplets will continue to break into smaller droplets. Aerodynamic drag on the droplets rapidly decelerates them and accelerates the gas entrained into the fuel spray. Evaporation and combustion of the fuel can be described using the model developed in Section 2.7. In some cases, however, pressures and temperatures in the cylinder are high enough that the liquid fuel is raised above its critical point. The fuel spray then behaves like a dense gas jet.

The entrainment of air into the unsteady, two-phase, variable-density, turbulent jet has been described by a variety of empirical models, simple jet entrainment models, and detailed numerical simulations. The problem is frequently complicated further by the use of swirling air motions to enhance mixing and entrainment. The swirling air motion sweeps the fuel jet around the cylinder, spreading it and reducing impingement on the cylinder wall. Since combustion in nonpremixed systems generally occurs predominantly at equivalence ratios near unity, combustion will occur primarily on the perimeter of the jet. Mixing of hot combustion products with the fuel-rich gases in the core of the fuel spray provides the environment in which large quantities of soot can be readily generated. (We discuss soot formation in Chapter 6.) The stoichiometric combustion results in high temperatures that promote rapid NO_x formation in spite of operation with large amounts of excess air in the cylinder under most operating conditions. Some of the fuel mixes with air to very low equivalence ratios before any of the mixture ignites. Temperatures in this region may be high enough for some fuel decomposition

and partial oxidation to occur, accounting for the relative abundance of aldehydes and other oxygenates in the diesel emissions (Henein, 1976).

Thus we see that diesel engines exhibit all of the complications of steady-flow spray flames, in addition to being unsteady. To describe the formation of pollutants quantitatively would require the development of a probability density function description of the unsteady mixing process. While such models are being explored (Mansouri et al., 1982a,b; Kort et al., 1982; Siegla and Amann, 1984), the methods employed are beyond the scope of this book. We shall examine, instead, the general trends as seen in both experimental and theoretical studies of diesel engine emissions and emission control.

4.2.1 Diesel Engine Emissions and Emission Control

Relatively low levels of gaseous exhaust emissions are achieved by light-duty (automobile) diesel engines without the use of exhaust gas treatment usually applied to gasoline engines to achieve similar emission levels (Wade, 1982).

The species mole fractions in diesel exhaust are somewhat misleading because of the low and variable equivalence ratios at which diesel engines typically operate. At low-load conditions, the operating equivalence ratio may be as low as 0.2, so the pollutants are diluted significantly with excess air. Because the equivalence ratio is continually varying in normal use of diesel engines, and to facilitate comparison to other engines, it is more appropriate to report emission levels in terms of emissions per unit of output: g MJ^{-1} for stationary engines or heavy-duty vehicles or g km^{-1} for light-duty vehicular diesel engines.

Injection of the liquid fuel directly into the combustion chamber of the diesel engine avoids the crevice and wall quench that allows hydrocarbons to escape oxidation in carbureted engines, so hydrocarbon emissions from diesel engines are relatively low. Furthermore, diesel engines typically operate fuel-lean, so there is abundant oxygen to burn some of the hydrocarbons and carbon monoxide formed in midair in the cylinder. NO_x emissions from prechamber diesel engines are lower than the uncontrolled NO_x emissions from homogeneous charge gasoline engines (Wade, 1982). The low NO_x emissions result from the staged combustion in the prechamber diesel and the inhomogeneous gas composition. Particulate emissions from diesel engines tend to be considerably higher than those of gasoline engines and represent a major emission control challenge.

Factors that influence the emissions from diesel engines include the timing and rate of fuel injection, equivalence ratio, compression ratio, engine speed, piston and cylinder design, including the use of prechambers, and other design factors. The influence of the overall equivalence ratio on engine performance is shown in Figure 4.28(a). The brake mean effective pressure increases with equivalence ratio, so higher equivalence ratios correspond to higher engine power output or load. The exhaust gas temperature also increases with equivalence ratio. Fuel consumption is high at low equivalence ratio, but decreases sharply as the equivalence ratio is increased. As the equivalence

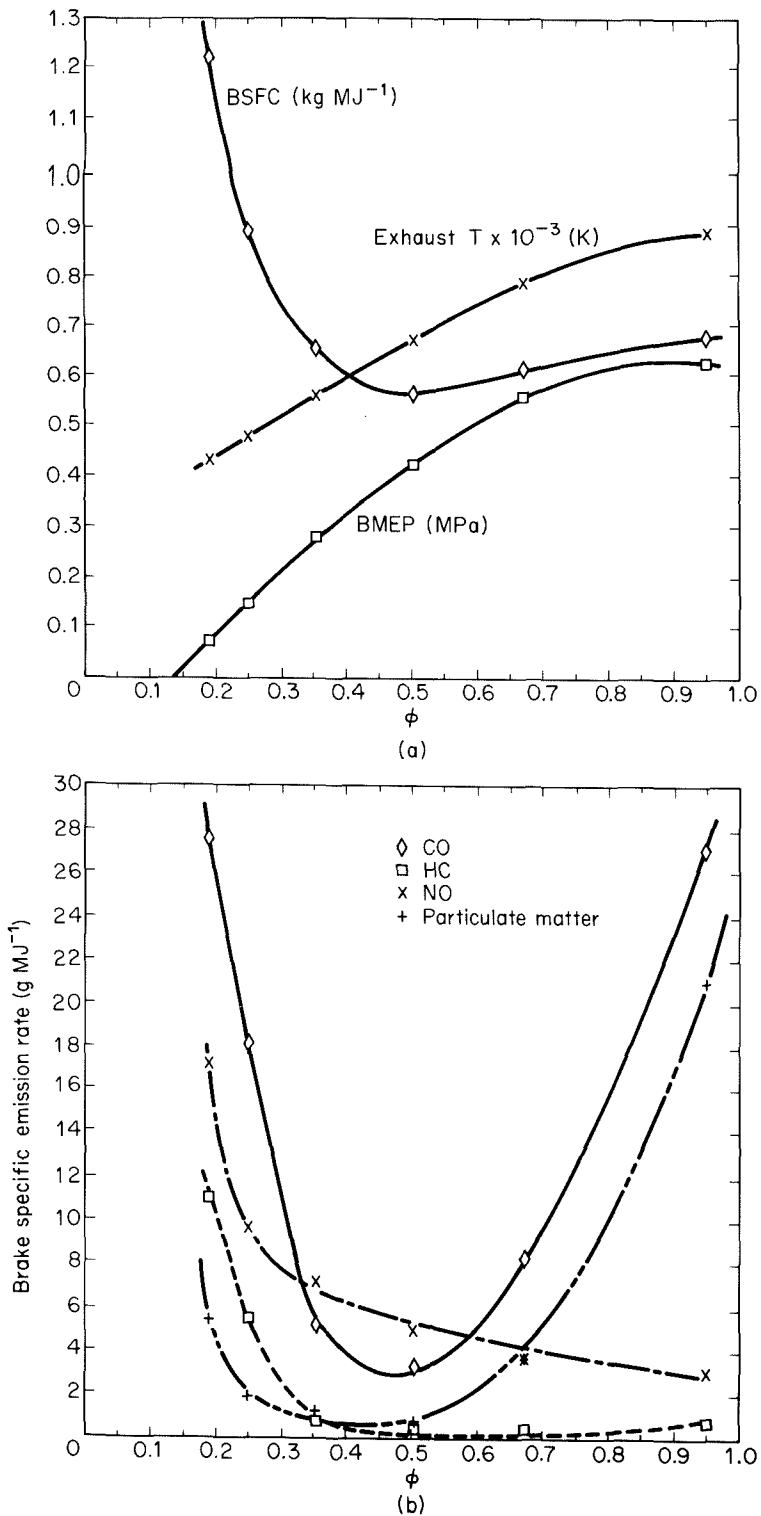


Figure 4.28 Influence of equivalence ratio on diesel engine performance and emissions (Wade, 1982; © SAE, Inc.).

ratio approaches unity, the fuel consumption increases slightly above a minimum value at about $\phi = 0.5$.

The variation of emissions with equivalence ratio is shown in Figure 4.28(b). In terms of grams emitted per MJ of engine output, all of the emissions are high at low equivalence ratios for which the engine output is small. Carbon monoxide and particulate emissions drop sharply with increasing equivalence ratio, pass through a minimum at about $\phi = 0.5$, and then rise sharply as ϕ approaches unity. Hydrocarbon and nitrogen oxide emissions, on the other hand, drop sharply as ϕ is increased above about 0.2, reaching relatively low levels at an equivalence ratio of about 0.4, and changing only slightly thereafter. It should be noted that, while the brake specific emissions of the latter pollutants decrease with increasing load, the absolute emission rate may increase at high power output.

While CO and hydrocarbon levels in diesel exhausts are quite low, particulate emissions from diesel engines are considerably higher than those from comparable spark ignition engines. The high particulate emissions are a consequence of the direct injection of fuel into the cylinder or prechamber of the diesel engine. The mixing is relatively slow, allowing some of the fuel to remain in hot, fuel rich gases long enough for polymerization reactions to produce the high-molecular-weight hydrocarbons that ultimately form carbonaceous particles known as soot. Subsequent mixing is slow enough that many of the particles escape oxidation in spite of the large amount of excess air that is typically available in the diesel engine. NO_x levels are also high because combustion in the turbulent diffusion flame of the diesel engine takes place in regions that are near stoichiometric. Because the diesel engine generally operates very fuel lean, reduction catalysts are not a practical solution to the NO_x emission problem. The exhaust temperature varies considerably with load and is on the low side for noncatalytic reduction by ammonia. Thus, until a feasible system for removing NO_x from diesel exhausts is developed, diesel NO_x control strategies must be based on modification of the combustion process. As with the spark ignition engine, penalties in fuel economy or engine performance may result. Moreover, efforts to improve the fuel economy or performance may aggravate the emission problem.

Diesel NO_x emissions result from the thermal fixation of atmospheric nitrogen, so control of these emissions can be achieved by reducing the peak flame temperatures. Equivalence ratio has, as we saw in Figure 4.28, relatively little influence on NO_x emissions from the diesel engine. The diffusion flame allows much of the combustion to take place at locally stoichiometric conditions regardless of the overall equivalence ratio. The peak temperatures can be reduced, however, through exhaust gas recirculation or retarding the injection timing. Exhaust gas recirculation in the diesel engine serves the same purpose as in the spark ignition engine: that of reducing the peak flame temperature through dilution with combustion products. Like spark retard, injection timing delays cause the heat release to occur late in the cycle, after some expansion work has occurred, thereby lowering the peak temperatures. The influence of these two control strategies on emissions and performance of an indirect injection automotive diesel engine is shown in Figure 4.29. Below about 30 percent exhaust gas recirculation, hydrocarbon, carbon monoxide, and particulate emissions are not significantly influenced by exhaust gas re-

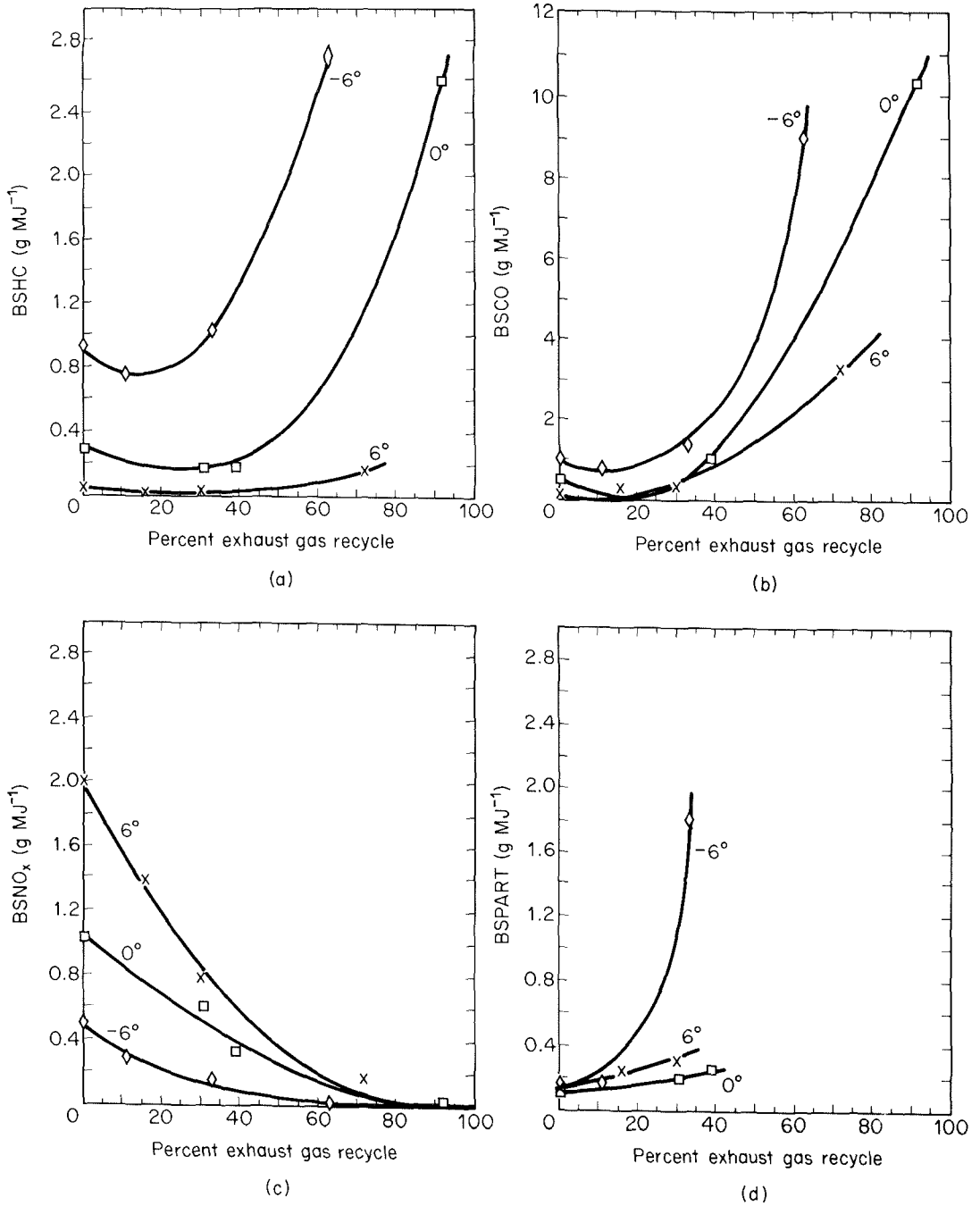
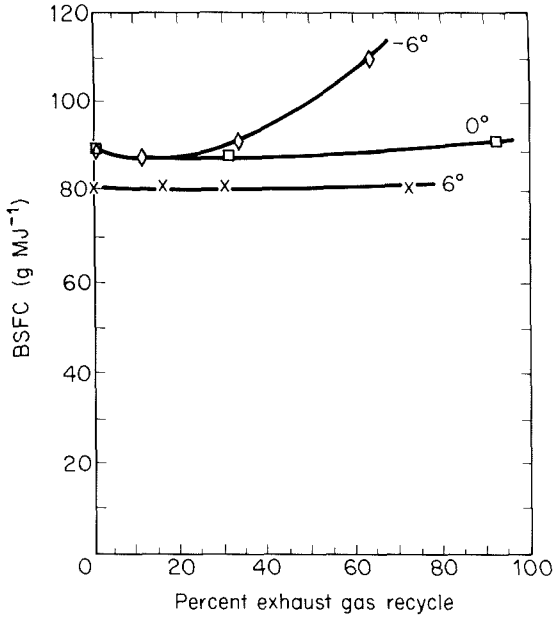


Figure 4.29 Influence of exhaust gas recirculation and injection timing on diesel engine performance and emissions (Wade, 1982; © SAE, Inc.).



(e)

Figure 4.29 (Cont.)

circulation, at least for the baseline fuel injection timing (denoted by 0°). NO_x emissions, on the other hand, are dramatically reduced by this level of EGR. As the amount of recycled exhaust gas is increased further, hydrocarbon and carbon monoxide emissions rise sharply, an indication that temperatures are too low for the combustion reactions to go to completion within the available time. Exhaust gas recirculation has, at least in this case, little effect on fuel consumption. Retarding the injection by 6 crank angle degrees from the baseline operation dramatically reduces NO_x emissions, but as might be expected when combustion is delayed in a mixing limited system, this reduction is accompanied by a marked increase in the emissions of hydrocarbons, carbon monoxide, and particulate matter. When accompanied by exhaust gas recirculation, injection retard leads to an increase in fuel consumption. Advancing the injection time reduces fuel consumption, emissions of hydrocarbons, and, to a lesser extent, emissions of carbon monoxide and particulate matter, but NO_x emissions increase.

Turbocharging is employed to improve engine efficiency and power. It has also been proposed as a technique that might reduce particulate emissions by providing more oxygen, possibly enhancing mixing and soot oxidation, and by increasing the intake temperature and thereby enhancing fuel vaporization. Turbocharging slows the increase in particulate emissions with increasing EGR and reduces both hydrocarbon emissions and fuel consumption. NO_x emissions, however, are increased by turbocharging. For a fixed level of NO_x emissions, the particulate emissions, unfortunately, are not significantly reduced by turbocharging. Moreover, at light loads, hydrocarbon emissions may actually increase with turbocharging.

Due to the relatively low nitrogen content of light diesel fuels, the formation of nitric oxide in the diesel engine is primarily by the thermal fixation of atmospheric nitrogen. Diesel engines can be operated, however, on heavier liquid fuels, or even on coal. The possible contributions of fuel-nitrogen to NO_x emissions must be considered for such operations.

4.2.2 Exhaust Gas Treatment

The diesel engine typically operates fuel-lean. The presence of excess oxygen in the combustion products suggests that the oxidation of carbon monoxide, hydrocarbon vapors, and carbonaceous particles in the exhaust gases may be possible. Wade (1980) examined the possibility of oxidizing the particles in the exhaust gases using a long exhaust reactor. At temperatures below 1000 K, the mass lost in 10 s due to oxidation was insignificant. At 1100 K, some mass was consumed by oxidation, but 3 s was required for an 80% reduction in the exhaust mass loading. Temperatures on the order of 1370 K would probably be required to achieve significant oxidation in a thermal reactor with a volume the same as the engine displacement. Thus oxidation of the particulate matter as it flows through an exhaust system does not appear to be a practical solution to the particulate emissions from vehicular diesel engines. The large temperature swings of the diesel exhaust temperature—in particular, the low temperatures encountered during low-load operation—make the thermal reactor impractical even for CO and hydrocarbon vapor emission control unless some additional fuel is added to raise the temperature.

An oxidation catalyst might be useful for the oxidation of carbon monoxide and hydrocarbons, particularly if it were effective in removing the condensible organics that contribute to the particulate emissions and the partially oxygenated hydrocarbons that are responsible for the diesel exhaust odor. The particulate matter deposition on the catalyst may affect the performance.

Filters or electrostatic precipitators can be used to remove particles from the exhaust gas stream, but disposal becomes a logistical problem in vehicular applications. These devices can be used, however, to concentrate the particulate matter for subsequent on-board incineration (Sawyer et al., 1982). After a sufficient quantity of particulate matter has been collected to sustain combustion, the collected carbonaceous material can be ignited by an auxiliary heat source and burned. This cleans the particle trap and allows extended operation without the buildup of such heavy deposits that engine back-pressure becomes a problem. A filter element may be impregnated with a catalyst to promote oxidation of the collected material at lower temperatures. Maintaining the trap at low temperature during the collection phase would facilitate the collection of vapors that would otherwise condense or adsorb on the soot particles upon release into the atmosphere. Periodic regeneration could be performed automatically using microprocessor control and sensors to monitor the status of the trap during the collection and regeneration phases of operation.

Filter elements may take the form of wire meshes, ceramic monoliths, or ceramic foams. Due to the wide range of temperatures and rapid changes to which the trap is exposed, the durability of these elements is a critical issue in the development of this

technology. If thermal shock leads to the development of cracks or fissures through which the exhaust can flow, the collection efficiency may be seriously degraded.

Reduction of NO_x in diesel exhaust gases represents a formidable challenge. Three-way catalysts are not effective because of the large amount of excess oxygen. The exhaust temperature varies over too wide a range for the noncatalytic ammonia injection technique to be useful, and the soot particles in the diesel exhaust are likely to foul or poison catalysts in the catalytic ammonia injection unless very effective particle removal is achieved. Alternative reducing agents that work at lower temperature, such as isocyanic acid (Perry and Siebers, 1986), may ultimately prove effective in diesel engine NO_x emission control.

4.3 STRATIFIED CHARGE ENGINES

The emphasis in our discussion of spark ignition engines has been on the homogeneous charge engines. The range of equivalence ratios over which such engines can operate has been seen to be very narrow due to the low laminar flame speed in rich or lean mixtures. The diesel engine, on the other hand, can operate at very low equivalence ratios. Soot formation in the compression ignition engine remains a serious drawback to its use.

An alternative approach that is intermediate between these two types of reciprocating engines is a stratified charge engine. Stratified charge engines rely on a spark for ignition as in the homogeneous charge engine, but utilize a nonuniform fuel distribution to facilitate operation at low equivalence ratios. The concept of the stratified charge engine is not new. Since the 1930s attempts have been made to develop hybrid engines that incorporate the best features of both the spark ignition and diesel engines (Heywood, 1981). Some, like the diesel, involve direct injection of the fuel into the cylinder. In others, two carbureted fuel-air mixtures are introduced into the cylinder, a rich mixture into a small prechamber and a lean mixture into the main cylinder.

Figure 4.30 illustrates the latter type of engine. The idea behind the prechamber stratified charge engine is that the fuel-rich mixture is easier to ignite than is the lean

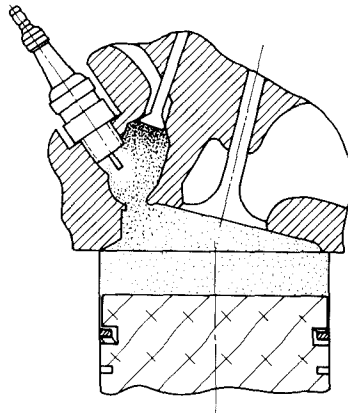


Figure 4.30 Prechamber stratified charge engine.

mixture in the main cylinder. The spark ignites the mixture in the prechamber. As it burns, the rich mixture expands, forming a jet through the orifice connecting the two chambers. The high-velocity flow of hot combustion products rapidly mixes with and ignites the lean mixture in the main cylinder. By this route, only a small fraction of the combustion takes place near stoichiometric, with most occurring well into the fuel-lean region. Thus NO_x formation is substantially slower than in a homogeneous charge engine.

The simplest conceptual model for the prechamber stratified charge engine is to assume that the mixture in the prechamber is uniform at a high equivalence ratio and that the mixture in the main cylinder is uniform at a lower value of ϕ . This assumption, however, is rather tenuous. During the intake stroke, the two mixtures flow through the two intake valves. Because of the large displacement volume, some of the prechamber mixture may flow out through the connecting orifice into the main chamber during intake. In the compression stroke, gas from the main chamber is forced back into the prechamber, so the prechamber will contain a mix of the rich and lean charges. Some of the prechamber mixture will remain in the main chamber. Thus, in spite of using carburetors to prepare the two charges, the two mixtures may not be uniform at ignition. During combustion, further mixing between the two gases takes place.

Analysis of gas samples collected at the exhaust port suggests that no significant stratification of the mixture remains at the end of the expansion stroke. This does not mean, however, that the gas is uniformly mixed on the microscale. As in the diesel engine, the turbulent mixing process plays a critical role in determining the pollutant emission levels. The dependence of the emissions from the prechamber stratified charge engine on equivalence ratio, as a result, is somewhat weaker than that of the conventional homogeneous charge engine. The reduction in the peak NO_x emissions with this technology is modest, but the ability to operate at very low equivalence ratios makes significant emission reductions possible.

Other types of stratified-charge engines utilize direct injection of the fuel into the cylinder to create local variations in composition. The fuels used in such engines generally still have the high-volatility characteristics of gasoline, and a spark is used for ignition. Two types of direct-injection stratified-charge engines are shown in Figure 4.31. The early injection version of the direct-injection stratified-charge engine typically uses a broad conical spray to distribute the fuel in the central region of the cylinder, where the piston has a cup. The spray starts early, about halfway through the compression stroke, to give the large fuel droplets produced by the low-pressure injector time to evaporate prior to ignition. In contrast, a late injection engine more closely resembles a diesel engine. A high-pressure injector introduces a narrow stream of fuel, beginning just before combustion. A swirling air motion carries the spray toward the spark plug.

The details of combustion in these engines are not well understood. Mixing and combustion occur simultaneously, so the dependence of emissions on equivalence ratio more closely resembles the weak dependence of poorly mixed steady-flow combustors than that of the conventional gasoline engine. Because pure fuel is present in the cylinder during combustion, the direct-injection stratified-charge engines suffer from one of the major difficulties of the diesel engine: soot is formed in significant quantities.

These are but a few of the possible configurations of reciprocating engines. The

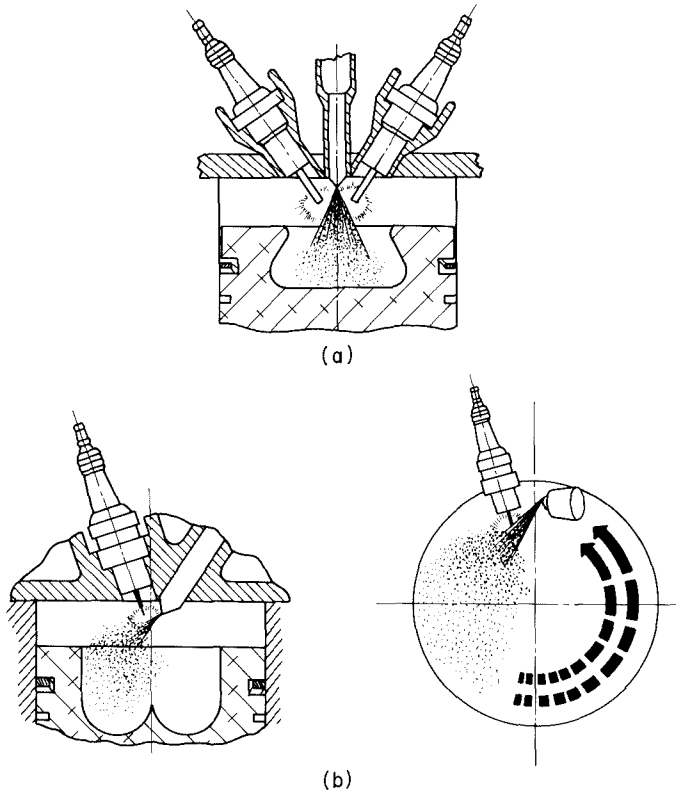


Figure 4.31 Direct-injection stratified-charge engine: (a) early-injection; (b) late-injection.

introduction of emission limitations on automobile engines has led to major new technological developments, some successful, many that failed to meet their developers' expectations. Renewed concern over engine efficiency has once again shifted the emphasis. To satisfy both environmental and fuel utilization constraints, the use of computer control, catalytic converters, and exhaust gas sensors has been introduced. These have diminished the level of interest in stratified charge engines, since NO_x reduction catalysts are needed to meet strict emission limits and require operation near stoichiometric. The problems of emission control for heavy-duty engines remain unresolved. Yet, as automobile emissions are reduced, large engines in trucks, railway engines, compressors, and so on, are becoming increasingly important sources of atmospheric pollutants, notably NO_x and soot.

4.4 GAS TURBINES

The fourth major class of internal combustion engines is the gas turbine. The power output of the gas turbine engine can be very high, but the engine volume and weight are generally much smaller than those of reciprocating engines with comparable output. The

original application of the gas turbine engine was in aircraft, where both weight and volume must be minimized. The high power output also makes the gas turbine attractive for electric power generation. Like reciprocating engine exhaust, the exhaust gases from the gas turbine are quite hot. The hot combustion products can be used to generate steam to drive a steam turbine. High efficiencies of conversion of fuel energy to electric power can be achieved by such combined-cycle power generation systems. Clearly, the constraints on these applications differ greatly, so the technologies that can be applied to control emissions for one type of gas turbine engine are not always applicable to the other.

Unlike the reciprocating engines, the gas turbine operates in steady flow. Figure 4.32 illustrates the main features of a gas turbine engine. Combustion air enters the turbine through a centrifugal compressor, where the pressure is raised to 5 to 30 atm, depending on load and the design of the engine. Part of the air is then introduced into the primary combustion zone, into which fuel is sprayed and burns in an intense flame. The fuel used in gas turbine engines is similar in volatility to diesel fuel, producing droplets that penetrate sufficiently far into the combustion chamber to ensure efficient combustion even when a pressure atomizer is used.

The gas volume increases with combustion, so as the gases pass at high velocity through the turbine, they generate more work than is required to drive the compressor. This additional work can be delivered by the turbine to a shaft, to drive an electric power generator or other machinery, or can be released at high velocity to provide thrust in aircraft applications.

The need to pass hot combustion products continuously through the turbine imposes severe limits on the temperature of those gases. Turbine inlet temperatures are limited to 1500 K or less, depending on the blade material. The development of turbine blade materials that can withstand higher temperatures is an area of considerable interest because of the efficiency gains that could result. In conventional gas turbine engines, the cooling is accomplished by dilution with additional air. To keep the wall of the combustion chamber, known as the combustor can, cool, additional air is introduced through wall jets, as shown in Figure 4.33. The distribution of the airflow along the length of the combustion chamber, as estimated by Morr (1973), is also shown.

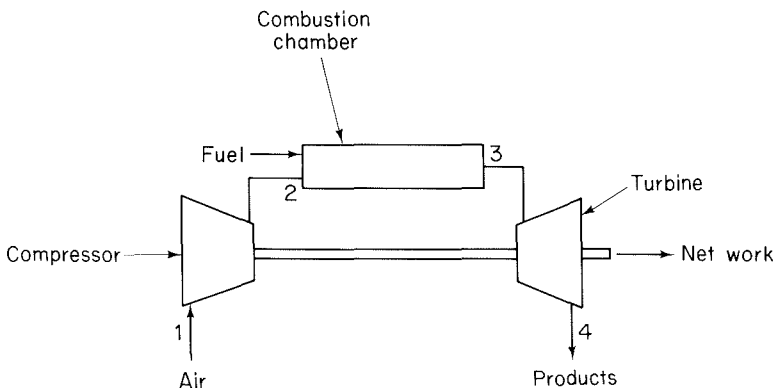


Figure 4.32 Gas turbine engine configuration.

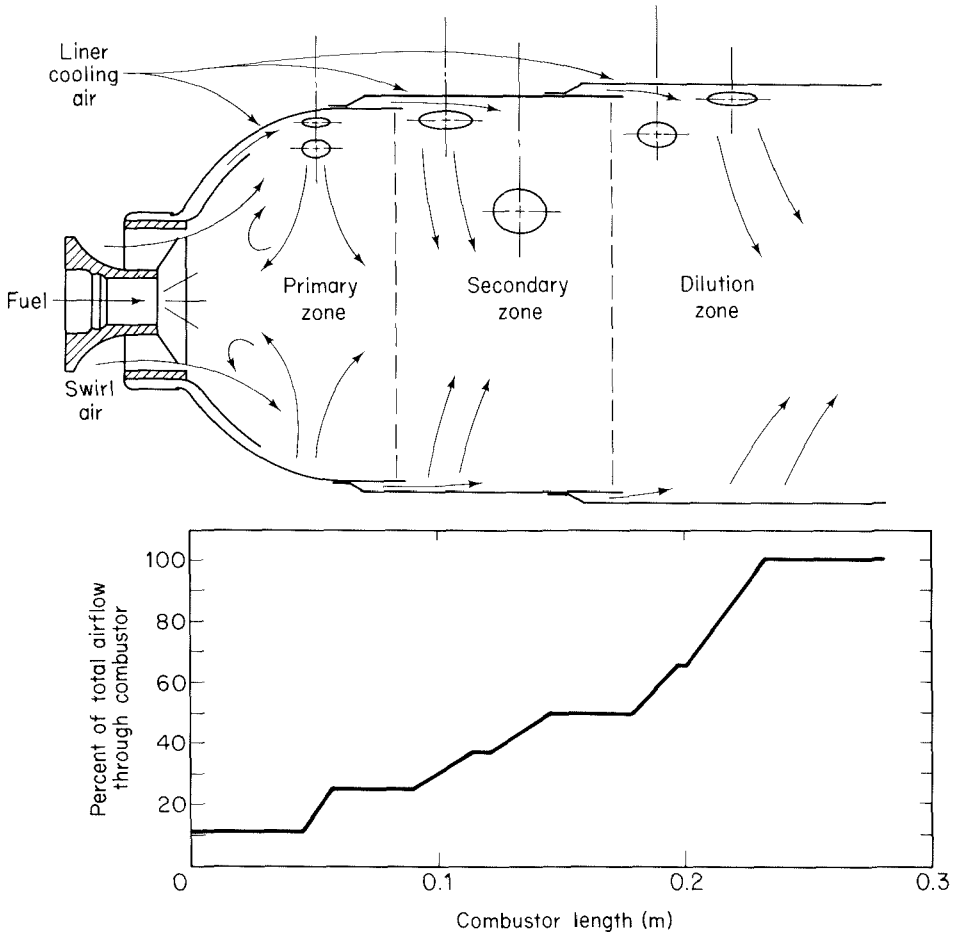


Figure 4.33 Gas turbine combustion, airflow patterns, and air distribution. Morr (1973).

Size and weight limitations are severe for aircraft applications. Even for stationary gas turbines, the engine size is limited due to the high operating pressures, although the constraints are not nearly as severe as in aircraft engines. Thus the residence time in the gas turbine is generally small, on the order of several milliseconds. Flame stability is also of critical importance, particularly in aircraft engines. Recirculation caused by flow obstructions or swirl is used to stabilize the flame.

The combustion environment in gas turbine engines varies widely with load. At high load, the primary zone typically operates at stoichiometric. The high-velocity gases leaving the combustor drive the turbine at a high rate, so the pressure may be raised to 25 atm. Adiabatic compression to this level heats the air at the inlet to the combustion chamber to 800 K. Air injected into the secondary combustion zone reduces the equivalence ratio to about 0.5. As this air mixes with the burning gases, combustion ap-

proaches completion. Finally, dilution air reduces the equivalence ratio to below 0.3, lowering the mean gas temperature to the turbine inlet temperature of less than 1500 K.

At idle, the pressure may only increase to 1.5 atm, so the inlet air temperature is not significantly greater than ambient. The equivalence ratio in the primary combustion zone may be as low as 0.5, resulting in a mean gas temperature of only 1100 K. The distribution of air in the different regions of an aircraft engine is determined by the combustion can geometry and therefore does not change with load. The combustion products at idle may be diluted to an equivalence ratio below 0.15 at the turbine inlet, lowering the mean gas temperature to below 700 K.

Because of the very short residence time in the combustion chamber, droplet evaporation, mixing, and chemical reaction must occur very rapidly. The short time available profoundly influences the pollutant emissions from gas turbine engines. As illustrated in Figure 4.34, at low load, when the overall equivalence ratio is well below unity and the gases are rapidly quenched, NO_x emissions are low. These same factors cause the CO and hydrocarbon emissions to be high in low-load operation. At high load, on the other hand, the gases remain hot longer and the equivalence ratio is higher, so more NO_x is formed; while CO and hydrocarbon oxidation is more effective at high loads, causing emissions of these species to decrease with load. Soot, however, is also formed in the gas turbine engine at higher loads due to the imperfect mixing, which allows some very fuel-rich mixture to remain at high temperatures for a relatively long time.

Gas turbine engines used for electric power generation and other applications where weight is not so critical introduce additional factors into the emissions problem. While aircraft engines generally burn distillate fuels with low sulfur and nitrogen contents, stationary gas turbines frequently burn heavier fuels. Fuel-bound nitrogen may contrib-

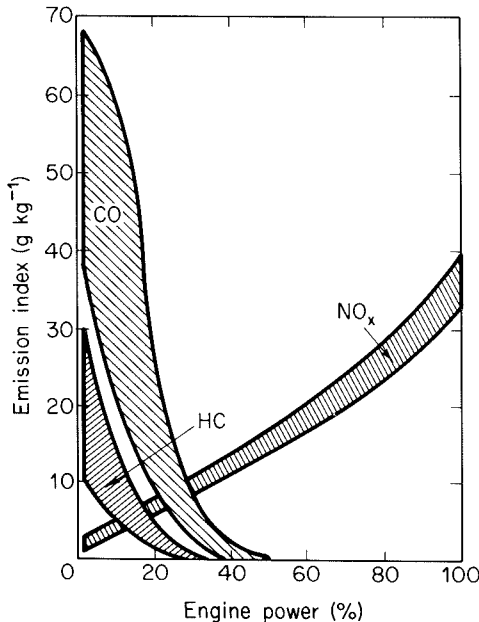


Figure 4.34 Variation of gas turbine engine emissions with engine power.

ute significantly to NO_x emissions, and sulfur oxides may be emitted as well. The use of coal directly or in combination with a gasifier could aggravate these problems and also introduce the possibility of fine ash particles being emitted. (Coarse ash particles are less likely to be a problem. Because their presence would rapidly erode the turbine and significantly degrade its performance, large particles must be efficiently removed from the combustion products upstream of the turbine inlet.)

In contrast to most other steady-flow combustors, NO_2 levels can be comparable to or even exceed NO levels in the exhaust gases, as shown in Figure 4.35. Rapid quenching of the combustion products has another effect: promoting the formation of large concentrations of NO_2 .

The control of emissions from gas turbine engines involves a number of factors:

1. *Atomization and mixing.* Poor atomization and imperfect mixing in the primary combustion zone allow CO and unburned hydrocarbons to persist into the secondary zone, where the quenching occurs. It also allows stoichiometric combustion to take place even when the overall equivalence ratio of the primary zone is less than unity, thereby accelerating the formation of NO_x .
2. *Primary zone equivalence ratio.* To lower NO_x emissions at high load, it is necessary to reduce the peak flame temperatures. Since the overall equivalence ratio of the gas turbine engine operation must be so low, reducing the primary zone equivalence ratio is a promising approach. Of course, effective mixing is required at the same time.
3. *Scheduling of dilution air introduction.* By first diluting the combustion products to an equivalence ratio at which CO and hydrocarbon oxidation are rapid and then allowing sufficient time for the reaction before completing the dilution, it may be possible to complete the oxidation, even at low loads. The total combustor volume and the need to cool the combustion can walls limit the extent to which this can be accomplished.

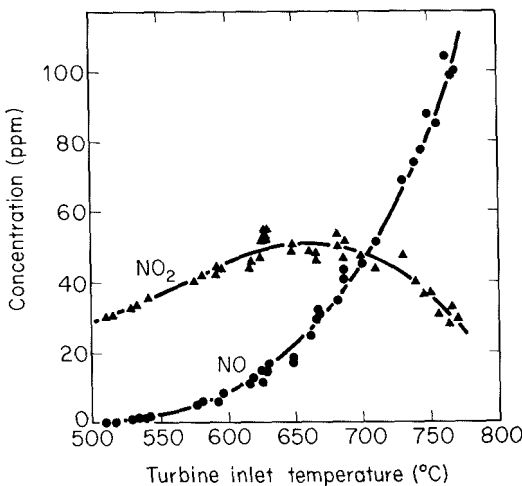


Figure 4.35 NO and NO_2 emissions from a gas turbine power generating unit (Johnson and Smith, 1978). Reprinted by permission of Gordon and Breach Science Publishers.

A variety of approaches are being taken to control gas turbine engine emissions. To optimize performance at both high and low loads, many designs employ a number of small burners that are operated at near-optimum conditions all the time. An extreme example is the NASA Swirl Can Combustor, which contains 100 to 300 small (100-mm diameter) swirl can combustor modules assembled in a large annular array (Jones, 1978). To vary the load, the number of burner modules that are supplied with fuel is changed. At low loads, the flame extends only a small distance downstream of the individual modules, and most of the excess air does not mix directly with the combustion products. At high loads, so many modules are supplied with fuel that the flames merge and fill the entire combustion can. For sufficiently high combustor inlet temperatures, this design has the effect of delaying the rise in CO and hydrocarbons to quite low equivalence ratios. NO_x emissions are low at low load and rise dramatically with equivalence ratio (load). The general trends in NO_x emissions are well represented by a segregation parameter, (2.70), of $S = 0.3$ to 0.4 , indicating the degree of inhomogeneity in the gas turbine combustor. This suggests that much of the NO_x is formed in locally stoichiometric regions of the flame.

Further improvements can be realized by changing the way the fuel is introduced into the combustion chamber to minimize the residence time at stoichiometric conditions. Air-assist atomizers generate turbulence in the primary combustion zone, thereby accelerating the mixing. Some new turbine designs even involve premixing of fuel and air. Flame stability becomes a serious issue in premixed combustion as the equivalence ratio is reduced, so mechanical redistribution of the airflow is sometimes introduced to achieve stable operation at low loads (Aoyama and Mandai, 1984).

Multiple combustion stages are also incorporated into low NO_x gas turbine designs (see Figure 4.36), allowing efficient combustion in one or more small burners at low load and introducing additional fuel into the secondary zone to facilitate high-load fuel-lean combustion.

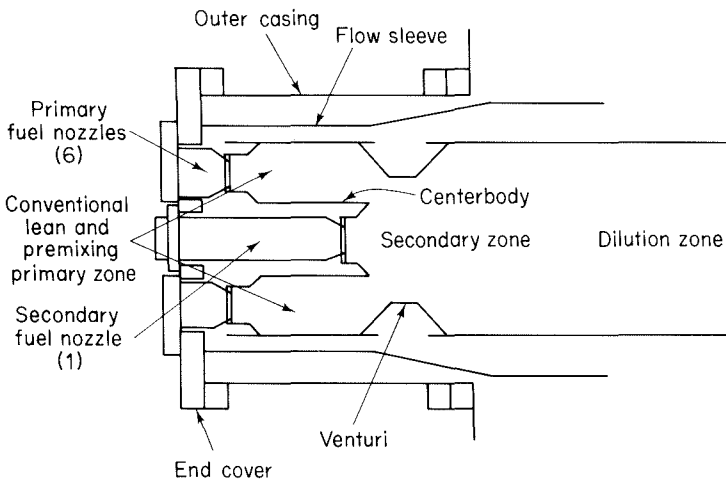


Figure 4.36 Staged combustion for a gas turbine engine (Aoyama and Mandai, 1984).

PROBLEMS

- 4.1.** An idealized thermodynamic representation of the spark ignition engine is the ideal-air Otto cycle. This closed cycle consists of four processes:
1. Adiabatic and reversible compression from volume $V = V_c$ to $V = V_c + V_d$
 2. Heat addition at constant volume, $V = V_c$
 3. Adiabatic and reversible expansion from $V = V_c$ to $V = V_c + V_d$
 4. Constant-volume ($V = V_c + V_d$) heat rejection
 - (a) Assuming that the ratio of specific heats, $\gamma = c_p/c_v$, is constant, derive an equation for the cycle efficiency ($\eta = \text{net work out/heat in during process 2}$) in terms of the compression ratio, R_c .
 - (b) Derive an expression for the indicated mean effective pressure (IMEP) in terms of the compression ratio and the heat transfer per unit mass of gas during process 2.
 - (c) Discuss the implications of these results for NO_x control by fuel-lean combustion and EGR.
- 4.2.** A chamber with volume, V , contains a mixture of octane and air at $\phi = 0.9$. The initial temperature and pressure are 298 K and 1 atm, respectively. The vessel may be assumed to be perfectly insulated.
- (a) The mixture is ignited and burned. Determine the final temperature and pressure.
 - (b) The pressure is measured as a function of time during the combustion process. Show how you would use the pressure measurements to determine the combustion rate. Plot the burned mass fraction as a function of the measured pressure.
- 4.3.** The vessel of Problem 4.2 is a 100-mm-diameter sphere. After complete combustion, a valve is suddenly opened to create a 10-mm-diameter sharp-edged orifice. The flow coefficient for the orifice is $C_f = 0.61$. Assuming the specific heats to be constant, calculate the pressure and temperature as a function of time while the vessel discharges its contents to the environment. What is the maximum cooling rate of the gas remaining in the vessel?
- 4.4.** Set up an engine simulation program based on the analysis of Section 4.1. For stoichiometric combustion of octane (assume complete combustion), calculate the pressure and the mean burned gas temperature as a function of crank angle for a compression ratio of $R_c = 8$, intake air pressure and temperature of 1 atm and 333 K (due to heating of the air in the intake manifold), and $\theta_i = -15^\circ$ and $\Delta\theta_c = 40^\circ$. Neglect heat transfer to the cylinder walls. Also calculate the mean effective pressure and the specific fuel consumption.
- 4.5.** A throttle reduces the pressure in the intake manifold to 0.6 atm. Assume that the flow to the throat of the valve is adiabatic and isentropic and that the pressure at the throat of the valve equals the pressure in the intake manifold. How much is the mass intake of air reduced below that for Problem 4.4? Using the cycle simulation code, repeat the calculations of Problem 4.4.
- 4.6.** Assuming the burned gases in Problem 4.4 are uniform in temperature, use the Zeldovich mechanism to calculate NO_x emissions from the engine.
- 4.7.** Use the engine simulation of Problem 4.4 to explore the effects of spark retard on engine performance (IMEP and ISFC) and on NO_x emissions.

- 4.8. A model that is commonly used to describe the recirculation zone of a combustor is the perfectly stirred reactor. The perfectly stirred reactor is a control volume into which reactants flow and from which products are continuously discharged. The reaction



proceeds with rate

$$R = -k_{+1}[A][B]$$

Assuming that the entering concentrations are $[A]_0$ and $[B]_0$, that the volume of the control volume is V , and that the volumetric flow rates into and out from the reactor are equal, $Q_{in} = Q_{out} = Q$, derive expressions for the steady-state concentrations of A and B .

- 4.9. Consider a gas turbine engine in which the incoming air is compressed adiabatically to a pressure of 6 atm. The airflow through the combustor at the design load is 3.5 kg s^{-1} . The fuel is aviation kerosene with composition $\text{CH}_{1.76}$ and a heating value of 46 MJ kg^{-1} . The combustor can is 150 mm in diameter and 300 mm long. The primary combustion zone is a 100 mm long perfectly stirred reactor (see Problem 4.9) operated at $\phi = 0.7$. Downstream of the primary reaction zone, dilution air is added to reduce the gas temperature by lowering the overall equivalence ratio to 0.2. Assume that the dilution air is added at a constant amount of dilution per unit of combustion can length. Further assume that the composition at any axial position in the combustor is uniform. The entire combustor may be assumed to be adiabatic.
- What is the residence time in the primary combustion zone?
 - Use the Zeldovich mechanism to calculate the NO concentration in the gases leaving the primary combustion zone.
 - Calculate and plot the temperature and the flow time as functions of axial position in the dilution region.
 - What is the NO concentration at the end of the combustor? What is the NO_x emission index, g/kg fuel burned?

REFERENCES

- ADAMCZYK, A. A., and LAVOIE, G. A. "Laminar Head-On Flame Quenching—A Theoretical Study," SAE Paper No. 780969, Society of Automotive Engineers, Warrendale, PA (1978).
- ADAMCZYK, A. A., KAISER, E. W., and LAVOIE, G. A. "A Combustion Bomb Study of the Hydrocarbon Emissions from Engine Crevices," *Combust. Sci. Technol.*, *33*, 261–277 (1983).
- AOYAMA, K., and MANDAI, S. "Development of a Dry Low NO_x Combustor for a 120-MW Gas Turbine," *J. Eng. Gas Turbines Power*, *106*, 795–800 (1984).
- BLUMBERG, P., and KUMMER, J. T. "Prediction of NO Formation in Spark-Ignition Engines—An Analysis of Methods of Control," *Combust. Sci. Technol.*, *4*, 73–95 (1971).
- BORGNACKE, C., ARPACI, V. S., and TABACZYNSKI, R. J. "A Model for the Instantaneous Heat Transfer and Turbulence in a Spark-Ignited Engine," SAE Paper No. 800247, Society of Automotive Engineers, Warrendale, PA (1980).
- BY, A., KEMPINSKI, B., and RIFE, J. M. "Knock in Spark Ignition Engines," SAE Paper No. 810147, Society of Automotive Engineers, Warrendale, PA (1981).

- CARRIER, G. F., FENDELL, F., and FELDMAN, P. "Cyclic Adsorption/Desorption of Gas in a Liquid Wall Film," *Combust. Sci. Technol.*, 25, 9–19 (1981).
- DANIEL, W. A., and WENTWORTH, J. T. "Exhaust Gas Hydrocarbons—Genesis and Exodus," SAE Paper No. 486B, Society of Automotive Engineers, Warrendale, PA (1962).
- HAMBURG, D. R., COOK, J. A., KAISER, W. J., and LOGOTHETIS, E. M. "An Engine Dynamometer Study of the A/F Compatibility between a Three-Way Catalyst and an Exhaust Gas Oxygen Sensor," SAE Paper No. 830986, Society of Automotive Engineers, Warrendale, PA (1983).
- HASKELL, W. W., and LEGATE, C. E. "Exhaust Hydrocarbon Emissions from Gasoline Engines—Surface Phenomena," SAE Paper No. 720255, Society of Automotive Engineers, Warrendale, PA (1972).
- HENEIN, N. A. "Analysis of Pollutant Formation and Control and Fuel Economy in Diesel Engines," *Prog. Energy Combust. Sci.*, 1, 165–207 (1976).
- HEYWOOD, J. B. "Pollutant Formation and Control in Spark-Ignition Engines," in *Fifteenth Symposium (International) on Combustion*, The Combustion Institute, Pittsburgh, PA 1191–1211 (1975).
- HEYWOOD, J. B. "Pollutant Formation and Control in Spark-Ignition Engines," *Prog. Energy Combust. Sci.*, 1, 135–164 (1976).
- HEYWOOD, J. B. "Automotive Engines and Fuels: A Review of Future Options," *Prog. Energy Combust. Sci.*, 7, 155–184 (1981).
- HEYWOOD, J. B., HIGGINS, J. M., WATTS, P. A., and TABACZYNSKI, R. J. "Development and Use of a Cycle Simulation to Predict SI Engine Efficiency and Nitric Oxide Emissions," SAE Paper No. 790291, Society of Automotive Engineers, Warrendale, PA (1979).
- HOULT, D. P., and WONG, V. W. "The Generation of Turbulence in an Internal Combustion Engine," in *Combustion Modeling in Reciprocating Engines*, J. N. Mattavi and C. A. Amann, Eds., Plenum Press, New York, 131–160 (1980).
- JOHNSON, G. M., and SMITH, M. Y. "Emissions of Nitrogen Dioxide from a Large Gas-Turbine Power Station," *Combust. Sci. Technol.*, 19, 67–70 (1978).
- JONES, R. E. "Gas Turbine Emissions—Problems, Progress, and Future," *Prog. Energy Combust. Sci.*, 4, 73–113 (1978).
- KAISER, E. W., LORUSSO, J. A., LAVOIE, G. A., and ADAMCZYK, A. A. "The Effect of Oil Layers on the Hydrocarbon Emissions from Spark-Ignited Engines," *Combust. Sci. Technol.*, 28, 69–73 (1982).
- KOMIYAMA, K., and HEYWOOD, J. B. "Predicting NO_x and Effects of Exhaust Gas Recirculation in Spark-Ignition Engines," SAE Paper No. 730475, Society of Automotive Engineers, Warrendale, PA (1973).
- KORT, R. T., MANSOURI, S. H., HEYWOOD, J. B., and EKCHIAN, J. A. "Divided-Chamber Diesel Engine: Part II. Experimental Validation of a Predictive Cycle-Simulation and Heat Release Analysis," SAE Paper No. 820274, Society of Automotive Engineers, Warrendale, PA (1982).
- KUMMER, J. T. "Catalysts for Automobile Emission Control," *Prog. Energy Combust. Sci.*, 6, 177–199 (1980).
- LAVOIE, G. A., HEYWOOD, J. B., and KECK, J. C. "Experimental and Theoretical Study of Nitric Oxide Formation in Internal Combustion Engines," *Combust. Sci. Technol.*, 1, 313–326 (1970).
- LAVOIE, G. A., LORUSSO, J. A., and ADAMCZYK, A. A. "Hydrocarbon Emissions Modeling for Spark Ignition Engines," in *Combustion Modeling in Reciprocating Engines*, J. N. Mattavi and C. A. Amann, Eds., Plenum Press, New York, 409–445 (1980).

- LoRUSSO, J. A., KAISER, E. W., and LAVOIE, G. A. "In-Cylinder Measurements of Wall Layer Hydrocarbons in a Spark Ignited Engine," *Combust. Sci. Technol.*, 33, 75–112 (1983).
- MANSOURI, S. H., HEYWOOD, J. B., and RADHAKRISHNAN, K. "Divided-Chamber Diesel Engine: Part I. A Cycle-Simulation which Predicts Performance and Emissions," SAE Paper No. 820273, Society of Automotive Engineers, Warrendale, PA (1982a).
- MANSOURI, S. H., HEYWOOD, J. B., and EKCHIAN, J. A. "Studies of NO_x and Soot Emissions from an IDI Diesel Using an Engine Cycle Simulation," IMechE Paper No. C120/82 (1982b).
- MORR, A. R. "A Model for Carbon Monoxide Emissions from an Industrial Gas Turbine Engine," Ph.D. thesis in mechanical engineering, MIT (1973).
- PERRY, R. A., and SIEBERS, D. L. "Rapid Reduction of Nitrogen Oxides in Exhaust Gas Streams," *Nature*, 324, 657–658 (1986).
- SAWYER, R. F., DRYER, F. L., JOHNSON, J. R., KLIEGL, J. R., KOTIN, P., LUX, W. L., MYERS, P. S., and WEI, J. *Impacts of Diesel-Powered Light-Duty Vehicles: Diesel Technology*, National Academy Press, Washington, DC (1982).
- SIEGLA, D. C., and AMANN, C. A. "Exploratory Study of the Low-Heat-Rejection Diesel for Passenger-Car Application," SAE Paper No. 840435, Society of Automotive Engineers, Warrendale, PA (1984).
- TABACZYNSKI, R. J., HEYWOOD, J. B., and KECK, J. C. "Time-Resolved Measurements of Hydrocarbon Mass Flowrate in the Exhaust of a Spark-Ignited Engine," SAE Paper No. 720112, Society of Automotive Engineers, Warrendale, PA (1972).
- TAYLOR, C. F. *The Internal Combustion Engine in Theory and Practice*, MIT Press, Cambridge, MA (1966).
- WADE, W. R. "Light-Duty Diesel NO_x -HC-Particulate Trade-Off Studies," in *The Measurement and Control of Diesel Particulate Emissions: Part 2*, J. H. Johnson, F. Black, and J. S. MacDonald, Eds., Society of Automotive Engineers, Warrendale, PA, 203–222 (1982).
- WENTWORTH, J. T. "Piston and Piston Ring Variables Affect Exhaust Hydrocarbon Emissions," SAE Paper No. 680109, Society of Automotive Engineers, Warrendale, PA (1968).
- WENTWORTH, J. T. "The Piston Crevice Volume Effect on Exhaust Hydrocarbon Emissions," *Combust. Sci. Technol.*, 4, 97–100 (1971).